Recent Advances in Preferential Oxidation of CO Reaction over Platinum Group Metal Catalysts

Kuo Liu,[†] Aiqin Wang, and Tao Zhang*

State Key Laboratory of Catalysis, Dalian Institute of Chemical Physics, Chinese Academy of Sciences, 457 Zhongshan Road, Dalian 116023, People's Republic of China

ABSTRACT: Preferential oxidation of CO (PROX) is an important reaction for removing small amounts of CO to a parts-per-million level from the hydrogen-rich stream, which will be ultimately supplied as a fuel to polymer–electrolyte membrane fuel cells. The key to the application of PROX is to develop a highly active and selective catalyst that operates well in a wide temperature window (e.g., 80–180 °C) and has good resistance to CO_2 and steam. In the past decades, various catalyst formulations have been developed, among which platinum group metal catalysts, including Pt, Ru, and Ir—in particular, those modified with promoters such as alkali metals and reducible metal oxides—have received a great deal of attention for their significantly improved catalytic activities in the low-temperature range. In this minireview, the recent advances of the platinum group metal catalysts for the PROX reaction are summarized, including performances of unpromoted and promoted catalysts, reaction mechanisms, and kinetics. In addition, the important roles of hydroxyl groups in the PROX reaction are also discussed.

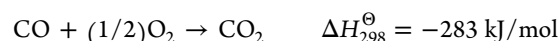**KEYWORDS:** platinum group metal catalysts, PROX, activity, mechanism, O_2 activation, OH groups
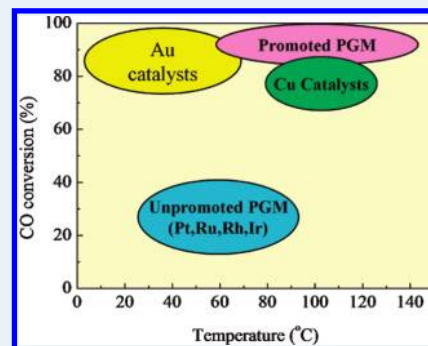
1. INTRODUCTION

The high demand for clean energy triggers the intensive interest in fuel cell-powered systems for stationary and mobile source applications. Among various types of fuel cells, the polymer–electrolyte membrane fuel cell (PEMFC), which operates typically around 80 °C with H^+ as a charge carrier, has been attracting much attention in the application to electric vehicles or residential power generations. The PEMFC possesses many attractive features, such as a low operating temperature, sustained operation at high current density, low weight, compactness, potential for low cost and volume, long stack life, rapid start-up, and suitability to discontinuous operation.[1] The PEMFC utilizes hydrogen as a fuel, and hydrogen is usually produced by autothermal reforming of hydrocarbons or alcohols (fuel + O_2 + H_2O ↔ CO_x + H_2), where without water, it is partial oxidation, and without oxygen, it is steam reforming and followed by the water gas shift reaction (CO + H_2O ↔ CO_2 + H_2) to eliminate most of the CO.[2-5]

The typical composition of effluent gas from the water gas shift reactor contains about 1% of CO in a large excess of H_2. However, the anode of PEMFC is prone to be poisoned by CO at low temperatures, even in the presence of small amounts of CO in the hydrogen stream.[6,7] Thus, carbon monoxide should be further removed to a trace level below 10 ppm.[8] During the past decade, great efforts have been put into the development of advanced technologies toward the selective removal of CO from H_2-rich reformate while minimizing the loss of H_2. Three approaches, including Pd-membrane separation,[9] catalytic methanation,[10] and preferential oxidation of CO in a large

excess of H_2 stream (PROX),[11,12] have been proposed and investigated intensively. Among the three purification methods, PROX appears to be the most promising one.

The PROX process involves two competitive reactions:

$$CO + (1/2)O_2 \rightarrow CO_2 \qquad \Delta H^{\ominus}_{298} = -283 \text{ kJ/mol}$$

$$H_2 + (1/2)O_2 \rightarrow H_2O \qquad \Delta H^{\ominus}_{298} = -242 \text{ kJ/mol}$$

Since the PROX operation unit is positioned between the low-temperature shift reactor (~200 °C) and the PEMFC (~80 °C), the catalyst for PROX should work between the two temperatures for the efficient use of energy. Meanwhile, start-up at low temperatures (e.g., room temperature) is also very important for the transportation application of fuel cells. Thus, an efficient PROX catalyst is required to exhibit good performances over a wide temperature range.[13]

The first patent for the PROX catalyst was awarded to Engelhard in the 1960s,[14] in which supported Pt catalysts were applied to purify the hydrogen for the application of ammonia synthesis. Later on, various catalysts were developed, with the aim of selectively removing CO while minimizing H_2 consumption in a wide operation temperature window (e.g., 80–180 °C) for the PEMFCs applications. According to the active metal used, the catalysts can be classified into group VIII metal catalysts (mainly platinum group metal catasts, denoted as PGM catalysts[15-19]) and group IB metal catalysts (Cu, Ag,

and Au-based catalysts[20−24]). On the other hand, the support materials have a great influence on the catalytic performance of metals, and can be classified into "inert" and "active" supports.[25]

Figure 1 gives a conceptual comparison of different types of metal catalysts for the PROX reaction. Supported gold catalysts
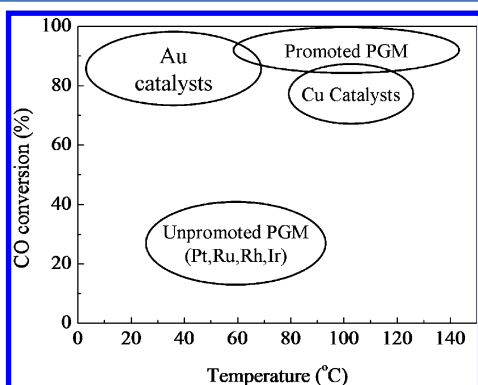

Figure 1. Conceptual illustration of catalytic performances of different types of catalysts for PROX reaction. For clarity, only the maximum CO conversion and reaction temperature window are shown, while the selectivity is not shown here.

are famous for their exceptionally high activity in low-temperature CO oxidation.[26−32] However, for the PROX reaction, there are very few gold catalysts that are able to remove CO to below 10 ppm in the targeted temperature range (e.g, 80−180 °C) because of the competitive oxidation of H_2 at elevated temperatures.[33−40] In addition, the deactivation trend of gold catalysts in a long operation term as well as their sensitivity to the preparation procedure also limits practical applications. In this context, supported gold catalysts may not be the best candidates for PROX applications. On the other hand, Cu-based catalysts, especially in combination with CeO_2 and Fe_2O_3, are usually active only above 100 °C and exhibit poor resistance toward water and CO_2.[41−50] Therefore, the Cu-based catalysts are also less attractive considering the practical PROX applications, although they are cost-effective.

In comparison with Au- or Cu-based catalysts, PGM catalysts (such as Pt, Ru, Ir, Rh catalysts)—in particular, reducible metal oxide-promoted Pt catalysts—give rise to very promising performances in the reaction temperature range 60−150 °C, as illustrated in Figure 1.[51−55] In the past decade, there have been intensive studies of the PROX reaction over promoted PGMs, including searching for more effective promoters, developing new advanced preparation methods, and clarifying the underlying mechanisms as well as kinetic studies. Especially, with the advancement of atomic resolution techniques as well as of theoretical calculation methods, the identification of active sites on the heterogeneous catalyst surface becomes possible. In this minireview, we give a summary of the recent advances of the PROX reaction over PGM catalysts, and the focus is put on the catalytic performances and the mechanisms of the reducible metal oxide-promoted PGM catalysts, since they have been considered as one of the most promising candidates used for practical hydrogen purification system connected to PEMFCs.

2. NONPROMOTED PGM CATALYSTS FOR THE PROX REACTION

Monometallic PGM catalysts such as Pt, Ru, Rh, and Ir on inert supports (named as nonpromoted PGM hereafter) usually give

very low activities at temperatures below 100 °C (see Figure 1). Noticeable PROX activities were observed only above 120 °C over these nonpromoted PGM catalysts.[56−59] Oh and Sinkevitch tested various PGM catalysts for the PROX reaction and reported that Ru/Al_2O_3 and Rh/Al_2O_3 were active for CO oxidation at 100 °C with a gas composition of 900 ppm CO, 800 ppm O_2, and 0.85% H_2 in N_2.[18] Nevertheless, this reaction condition is far from the practical application of PROX due to the very low concentration of hydrogen.

The supported Ru catalysts were found to be sensitive to preparation parameters such as Ru precursors, reducing agents, and pretreatment conditions, which significantly affected the activity and selectivity for the PROX reaction.[60−70] Chin et al.[60] prepared Ru/SiO_2 and Ru/Al_2O_3 catalysts by incipient wetness impregnation and observed that the use of a nitrate precursor and hydrogen reduction treatment resulted in finely dispersed Ru catalysts capable of completely eliminating CO in the temperature range 120−150 °C for Ru/SiO_2 and 160−180 °C for Ru/Al_2O_3. In contrast, Ru catalysts prepared from $RuCl_3$ precursor showed comparatively lower CO conversions, which was ascribed to the selective blockage of the active sites by Cl^- or Cl^--induced structural rearrangements. Addition of H_2O essentially had no effect on the CO oxidation over Ru/SiO_2, whereas a slightly negative effect was observed with Ru/Al_2O_3. On the other hand, the presence of CO_2 suppresses the CO oxidation over both catalysts at the high-temperature end.

Echigo's group[61−67] prepared Ru/Al_2O_3 by an impregnation method and made a comparative study between the prereduced and the nonreduced Ru catalysts. The result showed that over the prereduced Ru catalyst, CO was removed to below 10 ppm from the reformed gas between 85 and 170 °C at $[O_2]/[CO] = 1.5$ and between 90 and 140 °C at $[O_2]/[CO] = 1.0$, respectively, which were much wider than that of the nonreduced catalyst. Decreasing O_2/CO molar ratio resulted in an increasing outlet CO concentration and a narrow temperatue window. Moreover, Ru/Al_2O_3 showed good stability at 120 °C within 50 h in a reaction stream composed of 0.5% CO, 20% CO_2, 1.5% O_2, 6% N_2, 11% H_2O, and the balance H_2.[62]

Kim et al.[71] prepared 0.5 wt % $Ru/\gamma-Al_2O_3$ and 5 wt % $Ru/\gamma-Al_2O_3$ with a similar particle size distribution based on TEM analysis and found that the latter catalyst with a smaller amount of chemisorbed CO and O_2 per Ru metal showed much better PROX activity. In addition, Ru catalysts were reported to be stable for more than 10 000 h during the CO removal process.[65,66]

Han et al. reported that $Ru/\gamma-Al_2O_3$ showed excellent stability over 1000 min at 150 °C in a reformate gas mixture (1 kPa CO, 1 kPa O_2, 65 kPa H_2, and 10 kPa H_2O in CO_2).[72] The close correlation between the low-temperature PROX activity and the percent of Ru^0 was revealed by XPS study.[63] The CO conversion increased with an increase in the surface Ru^0 percent at low temperatures, but the selectivity for CO oxidation remained almost constant, regardless of the surface Ru^0 percent. It is supposed that the PROX activity of the Ru catalyst at low temperatures is dominated by O_2 activation on Ru^0, and the increase in the surface Ru^0 percent by the H_2/N_2 reduction leads to the high activity of the activated Ru catalyst. On the reduced Ru catalyst, two reactions contribute together to the CO removal,[68] including:

$$CO + 3H_2 \rightarrow CH_4 + H_2O$$

$$CO + (1/2)O_2 \rightarrow CO_2$$
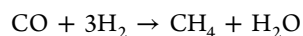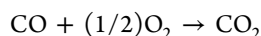
In addition to the above two reactions, Echigo et al.[62] also found that adding CO_2 into the feed mixture resulted in 100 ppm higher CH_4 concentration at 160 °C than that in the absence of CO_2, and the difference is wider at a higher temperature. Accordingly, the authors suggested that the methanation of CO_2 also occurred via the following reaction:

$$CO_2 + 4H_2 \rightarrow CH_4 + 2H_2O$$
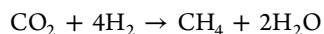
Nevertheless, the contribution of this reaction is very small in the low-temperature range (<180 °C).[62−64] Similar conclusions have also been drawn by Xu and Zhang.[73]

Specchia's group[74,75] prepared a series of Rh catalysts by an incipient wetness impregnation method, including Rh catalysts supported on A-type zeolites (**3A**, **4A**, and **5A**) Al_2O_3, TiO_2, and CeO_2. The results of the PROX reaction under the realistic conditions indicated that Rh catalysts supported on the reducible supports, such as CeO_2 and TiO_2, were comparatively less active at 80−120 °C than that on the inert supports. The most suitable catalyst for application operating at a temperature range compatible with the PEMFC is Rh-zeolite **3A**. In contrast with the pore sizes of **4A** and **5A** zeolite (4 Å and 5 Å, respectively), the pore size of **3A** zeolite (3 Å) was close to the diameter of the CO_2 molecules, which could make admittance of CO_2 into pores difficult and lower the CO_2 concentration on the active sites.

In addition, the different nature of the counterions, such as K^+, Na^+, and Ca^{2+}, may also have an effect on CO_2 affinity with the supports. Both effects relate to the enhancement of the PROX activity and the inhibition of the CO_2 methanation. It has also been found that an increase in the O_2 concentraion widened the temperature window for 100% CO conversion. The authors optimized the catalyst composition and the reaction conditions and came to the conclusion that 0.5% Rh-**3A** catalyst operating at $\lambda = 2O_2/CO = 3$ could reach 100% CO conversion in the temperature range from 80 to 120 °C at a constant space velocity 0.66 N L min^{-1} g$_{cat}^{-1}$, with no appearance of undesirable side reactions and at a possibly more acceptable cost for the reactor. In addition, the Rh catalyst supported on a mixture support of Al_2O_3 and **3A** zeolite was also reported to be a promising candidate for the PROX reaction.[76]

Ito et al.[77,78] found that adding niobia to Rh catalysts increased the activity and selectivity for the PROX reaction, and the activity was as follows: Rh/Nb_2O_5 > $Nb_2O_5−Rh/SiO_2$ > Rh/SiO_2 > $RhNbO_4/SiO_2$. Rh/Nb_2O_5 exhibited 100% CO conversion at 100 °C in a feed mixture of 0.2% CO, 3% H_2, and 1% O_2 after reductin at 500 °C. Han et al.[79] made a comparison among Rh/MgO, $Ru/\gamma-Al_2O_3$, and $Pt/\gamma-Al_2O_3$ catalysts in idealized methanol reformate (1 kPa CO, 1 kPa O_2, and 75 kPa H_2 in N_2) and pointed out that the activity of Rh/MgO at 250 °C exceeded that of the other two catalysts at their optimum temperatures by 2 orders of magnitude, indicating that Rh/MgO was a more active catalyst at temperatures higher than 250 °C.

Alumina-supporting monometallic Pt catalysts are perhaps the earliest studied catalysts, and typically, they have noticeable PROX activities above 150 °C.[80−82] Manasilp and Gulari[56] prepared Pt/Al_2O_3 catalyst by a sol−gel method and observed that 2% Pt/Al_2O_3 showed the maximum CO conversion (80%) at 170 °C with a selectivity of ~50%. Increasing the O_2 concentration from 0.5 to 1.35% increased the CO conversion

from 40−50% to 100% between 130 and 150 °C and decreased the selectivity from 55% to 35%. The presence of H_2O increased the activity over the whole temperature range of 110−190 °C by ~10-fold, and the activation energy was found to decrease from 74 to 37 kJ/mol after adding H_2O. Om contrast, the CO conversion decreased dramatically with the addition of CO_2 in the whole temperature range, and the maximum CO conversion dropped from 80 to 65% after adding CO_2. On the other hand, Avgouropoulos et al.[81] reported that Pt/Al_2O_3 could maintain 100% CO conversion for ~110 h at 100 °C in a reaction stream containing 1% CO, 1.25% O_2, 50% H_2, 15% CO_2, and the balance He. In addition, various zeolites were also employed as supports for Pt catalysts, such as ZSM-5,[83] A type and X type zeolites,[82,84] mordenite,[80,84] and Y type zeolite.[85,86]

Igarashi et al.[84] prepared a series of Pt/zeolite catalysts by an ion-exchange method, including Pt/A-zeolite, Pt/mordenite, Pt/X-zeolite, and Pt/Al_2O_3, and found that the zeolite-supported Pt catalysts exhibited a much higher selectivity than the alumina-supported ones in feed gas containing a large excess of hydrogen with the addition of a low concentration of oxygen (nearly 100% at 0.05% O_2). Pt/mordenite showed the highest conversion of CO to CO_2 among these catalysts, and Pt/A-zeolite catalysts exhibited the highest selectivity with the same CO conversion. In addition, a two-stage reactor was developed to achieve 100% CO conversion at 200 °C on the Pt/mordenite. The Pt catalysts supported on alkali metal-type zeolites, such as NaY, NaX, Na mordenite, KL zeolite, NaZSM-5, and Naβ zeolites were also claimed to be active for the PROX catalyst.[85]

Recently, Sebastian et al.[86] prepared different zeolitic material (MOR, ZSM-5, FAU, and ETS-10)-supported Pt catalysts. Among these catalysts, Pt/FAU had a larger pore size and volume than the other three zeolites, which led to a higher Pt dispersion. For Pt/ETS-10, Pt particles aggregated outside the microporous structure, in accordance with a low Pt dispersion and the low pore volume of ETS-10. Both Pt/FAU and Pt/ETS-10 exhibited high activity and selectivity for the PROX reaction when CO_2 or H_2O (or both) were also present in the reaction atmosphere, but Pt/FAU was the only one that could achieve 100% CO conversion below 180 °C.

By decreasing the oxygen content, both the selectivity and the temperature required to achieve a given CO conversion were increased on Pt/inert supports.[82,83] For example, Ren and Hong[80] found that if the O_2/CO decreased from 1.5 to 1, the temperature window for the parts-per-million level operation narrowed from 120−180 °C to 135−160 °C. Specchia's group prepared Pt-**3A** catalyst by an incipient wetness impregnation method, which showed a better performance than that prepared by an ion exchange method.[87,88] With this catalyst, the complete CO conversion and the maximum selectivity were obtained at 264 °C at a space velocity of 536 000 h^{-1} in the gas mixture, simulating water-gas shift (WGS) outlet composition (37% H_2, 5% H_2O, 18% CO_2, 0.5% CO, 0.75% O_2, and the rest He).[87]

From a more practical point of view, a structured catalyst may be a better choice than a powdered one. Specchia's group[89] deposited a mixed carrier of **3A**-zeolite and $\gamma-Al_2O_3$-supported Pt catalyst on the metal plates previously coated with $\gamma-Al_2O_3$, and the catalyst achieved complete CO conversion in the temperature range of 194−214 °C at GHSV = 2000 h^{-1} in a synthetic gas mixture simulating the WGS outlet composition (37% H_2, 5% H_2O, 18% CO_2, 0.5−1% CO, and 1−2% O_2 in

He). Rh catalyst deposited on a microreactor could also eliminate CO in a similar gas mixture in the temperature range of 120−180 °C.[90]

Until now, it has been difficult to compare strictly the activities of unpromoted PGM catalysts due to the broadly varied reaction conditions and preparation procedures. Nevertheless, Ru/Al_2O_3 catalyst appears as the most promising one for the PROX reaction among these catalysts on the basis of real operation data. Supported Ru catalysts are distinguished from other noble metal catalysts owing to their unique catalytic activities for CO/CO_2 methanation and reverse water gas shift reactions, which will consume additional H_2, accompanied by the removal of CO. The simultaneous consumption of H_2 reduces the scientific interest in developing this catalyst, although both oxidation and hydrogenation can be accomplished with one catalyst, which can provide a widened temperature range to achieve the acceptable CO removal. Other unpromoted monometallic noble metal catalysts, such as Rh, Pt, and Ir, were all suggested as bad candidates for the PROX reaction because they showed low activities at temperatures ranging from 80 to 120 °C (the operating temperature of PEMFCs) and low selectivities to CO_2 at higher temperatures. Over these catalysts, the use of a large excess of oxygen ($\lambda \geq 3$) was essential to achieve a 100% CO conversion, which would decrease the CO_2 selectivity and complicate the operation; therefore, the unpromoted PGM catalysts were not promising candidates for the PROX reaction. To increase the activities of the PGM catalysts at low reaction temperatures, promoters must be added. Here, the promoters indicate reducible metal oxides, alkali metal cations, or the second noble metal component, all of which have a remarkably promoting effect on the low-temperature activities of the PGM catalysts. The following part will focus on these promoted PGM catalysts.

3. PROMOTED PGM CATALYSTS FOR THE PROX REACTION

The conceptual illustration of Figure 1 clearly shows PGM catalysts modified by promoters exhibit greatly enhanced PROX activities in the operating temperature range of PEMFCs. To date, various promoters have been investigated, including reducible metal oxides either as the promoters or as the supports, the second noble metal that can form different bimetallic structures with the first PGMs, and alkali or alkali earth metal cations.

3.1. Bimetallic PGM Catalysts. Over the past few years, bimetallic catalysts have attracted much attention owing to their tunable chemical compositions and nanostructures, which in turn greatly affect the catalytic performances.[91−98] In particular, with the advancement in the synthesis of colloid metal nanoparticles, the size, morphology, and structure of bimetallic nanoparticles have become controllable to some extent,[99−102] which provides great opportunity for the development of high-performance bimetallic nanocatalysts. According to Eichhorn et al., the nanostructure of the bimetallic particles can be divided into core−shell, alloy, and linked monometallic nanoparticles.[103] Nevertheless, one must keep in mind that these structures may not be stable during the reaction, and some structural changes induced by the temperature and atmosphere[97,104] often occur, as illustrated in Figure 2. Therefore, in situ techniques must be employed in identifying the active sites.

Pt−Ru catalysts supported on alumina,[105] silica,[106] and mordenite[107] were reported to be superior to the monometallic
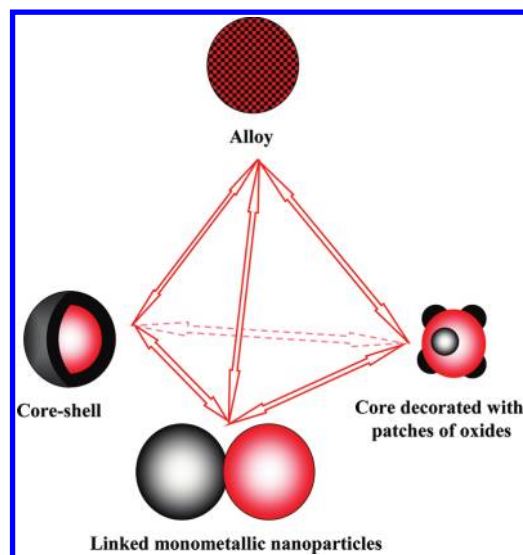

Figure 2. Different bimetallic structures and the possible transformations induced by pretreatment and reaction conditions. One metal is black and the other is red.

Pt catalyst. $Pt−Ru/Al_2O_3$, which was prepared by an impregnation method, showed 99% CO conversion and 62% selectivity at 100 °C, with a feed composition of 35% H_2, 17% CO_2, 28% N_2, 17% H_2O, 1% CO, and air as the oxidant, and by using a multistaged reactor system.[105] Chin et al.[106] prepared a $Pt−Ru/SiO_2$ catalyst by an incipient wetness coimpregnation method with a Ru/Pt atomic ratio of ∼2:1. The pretreatment of the $Pt−Ru/SiO_2$ catalyst by O_2/H_2 exhibited an activity between Pt/SiO_2 and Ru/SiO_2, whereas the pretreatment by H_2 resulted in a PROX activity similar to that of Ru/SiO_2. The prereduced $Pt−Ru/SiO_2$ by H_2 showed 100% CO conversion in the temperature range of 120−160 °C with 0.5% CO, 0.5% O_2, 45% H_2 in N_2.

Igarashi et al.[107] found that Pt−Ru/mordenite with a Pt/Ru atomic ratio of 2:1 showed 90% CO conversion and 90% CO_2 selectivity at 150 °C, with the gas mixture composed of 1% CO and 0.5% O_2 in H_2. Naknam et al.[108] also used a incipient wetness coimpregnation method to prepare Pt−Au/zeolite-A catalyst with a Pt/Au atomic ratio of 2. In this catalyst, Pt and Au appeared to be in separate phases. The Pt−Au catalyst has been found to be more active than the monometallic Pt catalyst, on which the temperature of 100% CO conversion has been shifted approximately 50 °C to a lower temperature. Furthermore, it was found that the Pt−Au catalyst exhibited good stability even in the presence of CO_2 and H_2O.

Parinyaswan et al.[109] prepared $Pt−Pd/CeO_2$ catalysts using a sol−gel method and found that the most active catalyst had a composition of Pt/Pd = 1/7. This catalyst showed ∼76% CO conversion at 90−110 °C, with a feed composition of 1% CO, 1% O_2, 4% CO_2, and 40% H_2 in He. However, CO conversion could be increased to ∼99% at 90 °C by increasing the O_2 concentraion to 2%. In addition, adding 10% H_2O in the feed gas could also increase the CO conversion to 85%. In contrast, CO_2 was reported to exert a detrimental effect on CO conversion. Increasing CO_2 concentration from 4% to 25% resulted in a decrease in the CO conversion from 76% to 50%.

Eichhorn and co-workers[103,110] reported a series of nano-particle (NP) catalysts made of a transition metal core (M = Ru, Rh, Ir, Pd, or Au) covered with a 1−2-monolayer-thick shell of Pt atoms. These catalysts were synthesized by using a

sequential polyol process. The core nanoparticles were first synthesized by reducing the corresponding metal precursors in refluxing glycol in the presence of polyvinylpyrrolidone stabilizer, and then the resulting core nanoparticles were coated with Pt through adding $PtCl_2$ to the core metal colloid. This synthesis procedure produced a PGM@Pt core−shell structure. Among the studied systems, Ru@Pt core−shell NPs exhibited significantly higher activity for the PROX reaction when compared with monometallic mixtures and bulk non-segregated bimetallic nanoalloys. The best Ru@Pt catalyst showed a 100% CO conversion below 20 °C (0.1% CO and 0.5% O_2 in H_2) and good stability.

3.2. Reducible Metal Oxide-Promoted PGM Catalysts.

Noble metals promoted with reducible metal oxides (denoted as MO_x hereafter) showed remarkable low-temperature activities in the PROX reaction. Among the reducible metal oxides, iron oxide is the most intensively studied promoter for noble metal catalysts owing to its outstanding promotional effect, especially in the temperature range 80−120 °C.

The work of Korotkikh and Farrauto[51] appears to be the first published study of supported PtFe catalysts for the PROX reaction. They found that with iron oxide promotion, CO conversion at 90 °C was increased significantly from 13.2% to 68.0% with a stoichiometric O_2/CO ratio and a pretty high weight hourly space velocity (WHSV = 150 000 L g^{-1} h^{-1}), but the selectivity remained relatively constant. Thereafter, many researchers studied the PtFe catalysts supported on zeolites, Al_2O_3 and SiO_2.

Watanabe et al.[52] developed a new Pt−Fe/mordenite catalyst by an ion-exchange method, and the activity of this catalyst was far superior to conventional Pt/Al_2O_3 and Pt/mordenite catalysts. A complete removal of CO with 100% selectivity was achieved by the addition of a stoichiometric amount of O_2 from a simulated reformate at 80−150 °C with a high gas hourly space velocity (GHSV = ~80 000 h^{-1}). Among various Pt/Fe ratios on a variety of zeolites, 4 wt % Pt−2 wt % Fe/mordenite gave the best activity and selectivity.[52] The Pt−Fe/mordenite catalyst could maintain 100% CO conversion for more than 20 h, even in the presence of CO_2 and H_2O.[54] Furthermore, supported PtFe catalysts could be washcoated on ceramic straight-channel monoliths[111,112] and metal foams.[113,114] Watanabe's group coated Pt−Fe/mordenite catalysts on ceramic straight-channel monoliths and demonstrated that the catalysts could achieve the 10-ppm target level at a low O_2/CO ratio (O_2/CO = 1) in a single-stage reactor. In addition, this catalyst exhibited excellent durability, since no deterioration in performance was observed during 500 h of operation.[111]

Bao's group[115] prepared a nanosized silica-supported PtFe catalyst, in which nanosized silica support was first function-alized with (3-aminopropyl)triethanoxysilane (APTES) fol-lowed by sequential deposition of Pt and Fe precursors. This synthesis procedure produced a structure with Fe patches on the surface of Pt particles. The resultant catalyst (4% Pt and 0.5% Fe) gave very high activity and selectivity for the PROX reaction with 100% CO conversion and 100% CO_2 selectivity at RT with a GHSV of 36 000 h^{-1}. Even at 80 °C, the CO conversion and CO_2 selectivity attained ~95%. More interesting, this catalyst showed 92% CO conversion and excellent stability under realistic PEMFC conditions when a considerable amount of CO_2 and H_2O was present. Under slight excess O_2 conditions, the CO can be removed, even to 1 ppm. With this catalyst assembled into a 1 kW PEMFC

working system, the cell performance remained stable for more than 900 h, which is in contrast to the deactivation after 30 min without the Pt−Fe catalyst.

Different from the above work in which Fe is added as a promoter in a small amount, our group used iron oxide directly as the support for the Pt catalyst. Surprisingly, at a low Pt loading (0.17 wt %), all the Pt species were dispersed as single atoms.[116] Aberration-corrected high-angle annular dark field scanning transmission electron microscopy (HAADF-STEM) and extended X-ray absorption fine structure (EXAFS) characterizations provide unambiguous evidence that Pt exists exclusively as single atoms on the whole catalyst without the presence of any clusters or particles. PROX activity tests showed that the single-atom catalyst Pt_1/FeO_x is 2−3 times more active than the cluster-sized catalyst, giving CO conversion of more than 95% at 80 °C at an extremely high GHSV of 11 000 000 mL g_{Pt}^{-1} h^{-1}. More interesting, this single-atom catalyst was rather stable in a 1000 min run at 80 °C, without any sintering or agglomeration. This unprece-dented high activity of Pt single atoms supported on FeO_x has an important implication of developing low-cost but highly active PROX catalysts.

The above iron oxide-promoted or -supported Pt catalysts were all prepared by simple impregnation, coprecipitation, or the ion-exchange method. An alternative approach to this type of catalysts is to use the colloid Pt−Fe bimetallic nanoparticles as precursors to get an improved interaction between Pt and Fe. Shen's group[117] prepared colloid Pt−Fe bimetallic nano-particles using a modified polylol method in which the Pt nanoparticles first were obtained and then acted as crystal nuclei for deposition of Fe. The as-prepared nanoparticles were deposited onto an Al_2O_3 support. It was found that the Pt−3Fe/Al_2O_3 gave a CO conversion of 99% and CO_2 selectivity of 98% at 30−80 °C at a GHSV of 10 000 h^{-1} and was stable at 80 °C within 50 h.[117] Our group also reported Pt−Fe/Al_2O_3 catalysts prepared with $Pt(acac)_2$ and $Fe(acac)_3$ as precursors and ethylene glycol as a soft reducing agent in Ar, which showed improved PROX activity over Pt/Al_2O_3.[118] Siani et al.[119] developed a cluster-derived PtFe/SiO_2 catalyst by using $PtFe_2(COD)(CO)_8$ and $Pt_5Fe_2(COD)_2(CO)_{12}$ organometallic cluster precursors. Compared with PtFe/SiO_2 prepared by conventional impregnation procedure, the cluster-derived catalysts possessed a high degree of metal dispersion and more homogeneous mixing of Pt and Fe and were therefore more active for the PROX reaction. However, this catalyst showed a slow deactivation during the PROX reaction.

In addition to iron oxide, other reducible oxides have also proved to be effective promoters for noble metal-catalyzed PROX reaction. For example, CeO_2-[120−125] as well as $Ce_xZr_{(1-x)}O_2$-[126−128] supported Pt catalysts were reported to be much more active than the Pt/Al_2O_3 catalyst in the low temperature range (60−100 °C). However, a complete conversion of CO was achieved only with an excess amount of O_2, which caused additional consumption of H_2. Thus, CO_2 selectivity is rather low at a total conversion of CO over CeO_2-supported Pt catalysts.

Sn was also reported to be an effective promoter for the Pt-catalyzed PROX reaction.[129−134] The carbon-supported Pt_3Sn catalyst showed lower activation energy for CO oxidation than that for H_2 oxidation, whereas Pt/Al_2O_3 catalyst had similar activation energies for both reactions that are larger than that on Pt_3Sn catalysts.[129] The influence of Sn was remarkable, increasing the catalytic activity of Pt atoms by 1 order of

magnitude. Furthermore, the presence of hydrogen was found to promote the rate of CO oxidation.[130,131] Pt supported on Nb_2O_5 catalysts presented higher activity than Pt/Al_2O_3 or $PtSn/Al_2O_3$ in the PROX reaction at low temperatures, but with a lower CO_2 selectivity.[132]

Both Co and Cu can form intermetallic compounds (IMCs) with Pt. Komatsu and Tamura reported that Pt_3Co and PtCu IMCs supported on silica functioned as active catalysts for PROX in the temperature range of 100−180 °C.[135] The Pt_3Co catalyst was more selective than PtCu for CO_2 formation. Characterizations suggested that the formation of IMCs induced elongation of the Pt−Pt bond distance and electron transfer from Pt to Co or Cu; both effects weakened CO adsorption and therefore increased the low-temperature activity.

The promotional role of Co was also found in other supported Pt catalysts, such as $Pt−Co/TiO_2$[136] and $Pt−Co/$$Al_2O_3$.[137] In particular, Pt−Co/YSZ (yttria-stabilized zirconia) with Pt/Co = 1/5 (0.5 wt % Pt) exhibited the best performance among various Pt−Co catalysts, which could reduce the CO concentration to below 10 ppm in the temperature range of 110−150 °C, even under practical conditions (containing both CO_2 and H_2O in the inlet gas).[138] Similar to the Pt−Co catalysts, Pt−Ni catalysts supported on Al_2O_3 or CNT (carbon nanotube) were also active and selective at low temperatures for the PROX reaction.[139−142] The maximum CO conversion could be obtained at 75 °C on Pt−Ni/CNTs, with the selectivity ∼50% in 1% CO, 1% O_2, 50% H_2, and N_2 (WHSV = 48 000 mL g_{cat}^{-1} h^{-1}). In addition, Pt−Ni/CNTs could maintain 100% CO conversion for ∼31 h in the absence of CO_2 and H_2O at 115 °C.[141] Surface science studies showed that the synergy arose from a sandwich structure consisting of surface Ni oxide nanoislands and subsurface Ni atoms at a Pt surface. The surface Ni oxide nanoislands activate O_2 to produce atomic O, and the subsurface Ni atoms promote the elementary reaction between CO and O.[142]

In contrast to the extensive studies on the Pt-based catalysts, Ir catalysts received less attention, probably because of their inferior activity. Recently, effective supported Ir catalysts have been prepared. Okumura et al.[15] prepared Ir/TiO_2 catalysts by deposition-precipitation and impregnation, both of which were proved to be active for CO oxidation after pretreatment in a stream of 20% H_2 in Ar at 250 °C for 1 h. These catalysts showed 100% CO conversion at room temperature with 1% CO in air at a space velocity of 20 000 mL g_{cat}^{-1} h^{-1}. Mariño and co-workers[120] were the first to report Ir/CeO_2 as an active catalyst for the PROX reaction. They used an expensive chlorine-free Ir precursor, $Ir[CH(COCH_3)_2]_3$, instead of inexpensive and easily available H_2IrCl_6 in the preparation of Ir/CeO_2 and $Ir/Ce_xZr_{(1−x)}O_2$ by means of impregnation. Ceria−zirconia-supported Ir and Pt catalysts showed a similar behavior; the same trends were observed for both catalysts, and a maximum appeared at ∼100 °C in the evolution of the CO conversion as a function of temperature, although the Ir catalyst was slightly less active than the Pt catalysts.

Our group performed an intensive study of Ir catalysts for thePROX reaction, including CeO_2-supporting Ir catalysts,[143−149] and Al_2O_3- and SiO_2-supporting Ir catalysts promoted with FeO_x.[150−155] It was found that deposition− precipitation (DP) with either NaOH or urea as the precipitation agent yielded highly active Ir/CeO_2 catalysts, whereas impregnation with Cl-containing precursor (H_2IrCl_6) gave a rather poor catalyst.[144] The underlying reason is that the

formation of Ce−O−Cl species inhibits the mobility of surface oxygen in the CeO_2 support. Among various supports investigated (CeO_2, TiO_2, Al_2O_3, and MgO), only CeO_2-supporting Ir catalysts were active for the low-temperature PROX reaction; the maximum CO conversion of ∼70% was obtained at 80 °C with a stoichiometric ratio of CO/O_2 at a GHSV of 40 000 h^{-1}.[143,144]

Since most of the Ir particles are on the surface of the CeO_2 support when a DP procedure is employed to produce the Ir/CeO_2 catalyst (denoted as Ir-on-CeO_2), this Ir-on-CeO_2 catalyst will be less selective for CO oxidation due to the competitive H_2 oxidation occurring on the exposed Ir surfaces. Therefore, we developed a new Ir-in-ceria catalyst in which most of the iridium particles are embedded in the ceria matrix through the redox reaction between Ce^{3+} and Ir^{4+} during coprecipitation.[145] The most attractive feature of this Ir-in-CeO_2 catalyst is the almost unchanged selectivity (over 70%) for CO oxidation over a wide temperature window (80−180 °C). Due to the absence of extensively exposed Ir species on the surface of the Ir-in-CeO_2 catalyst, H_2 oxidation occurring on the Ir species and the ceria support at high temperatures was significantly suppressed, thus keeping a high selectivity for CO oxidation, even at elevated temperatures. Making use of the different features of the two Ir/CeO_2 catalysts, we developed a dual bed system with the top Ir-in-CeO_2 and the bottom Ir-on-CeO_2.[146] This dual bed system is unique in affording a high CO conversion in a wide temperature window, from 80 to 200 °C, which is superior to a single bed catalyst.

In addition to Ir/CeO_2 catalysts, we also developed iron oxide-promoted Ir/Al_2O_3[150,151] and Ir/SiO_2[152−156] catalysts that were prepared by a simple impregnation method using H_2IrCl_6 and $Fe(NO_3)_3$ as the precursors. Similar to the iron oxide-promoted Pt catalysts, the $Ir−Fe/Al_2O_3$ and $Ir−Fe/SiO_2$ were also significantly more active than the nonpromoted counterparts for the low-temperature PROX. The IrFe catalyst showed a maximum CO conversion of ∼90% and CO_2 selectivity of ∼90% at 80 °C in 2% CO, 1% O_2, and 40% H_2 in He at a GHSV of 40 000 h^{-1}. Moreover, the impregnation sequence of Ir and Fe remarkably affected the activity; coimpregnation gave the best performance.[150−153] Interestingly, when we directly used $Fe(OH)_x$ as a support of Ir rather than as a promoter, the resulting catalyst exhibited an even higher activity in the PROX reaction.[156] CO conversion reached 100% at 20−40 °C on $Ir/Fe(OH)_x$ catalyst with a feed gas composition of 1% CO, 1% O_2, and 40% H_2 in He and a WHSV of 18 000 mL g_{cat}^{-1} h^{-1}. The calculated turnover frequency of the $Ir/Fe(OH)_x$ catalyst was at least 1 order of magnitude higher than other reported PGM catalyst systems.

3.3. Alkali Metal-Promoted PGM Catalysts. It was found that the addition of a suitable amount of alkali (Li, Na, K, Rb, Cs) or alkali earth metals (Mg) to the precious metal catalysts led to a significant increase in the PROX activity and selectivity.[157−163] Among various additives, the promotional effect of K is most remarkable. It was reported that when the atomic ratio of K/Pt = 10/1, the $K−Pt/Al_2O_3$ was 20 times as active as that of Pt/Al_2O_3 for the PROX reaction at 80 °C and was able to decrease the CO concentration below 10 ppm in the range of 100−140 °C.[158] Interestingly, it seems that the promotional effect of K is more pronounced on the inert-oxide-supported Pt catalysts than that on the reducible-oxide-supported ones. Tanaka et al.[162] observed that $K−Pt/Al_2O_3$ and $K−Pt/SiO_2$ exhibited a much higher CO conversion and CO_2 selectivity than $K−Pt/ZrO_2$, $K−Pt/Nb_2O_5$, and K−Pt/

TiO$_2$, and the high performance on the former catalysts was temporarily ascribed to the high BET surface areas of Al$_2$O$_3$ and SiO$_2$. In addition, adding H$_2$ or increasing the O$_2$ concentraion in the feed could enhance the CO oxidation rate much more dramatically on K−Pt/Al$_2$O$_3$ than Pt/Al$_2$O$_3$. The promotional role of H$_2$ has also been claimed on M−Pt/Al$_2$O$_3$ (M = Cs, Rb, Na, and Li);[159,161] however, the CO$_2$ selectivity on K−Pt catalyst declined slightly with an increase in the O$_2$ concentration in the feed.[162]

4. MECHANISTIC AND KINETIC STUDIES

4.1. The Mechanism of PROX on the Nonpromoted PGM Catalysts.
For the PROX reaction occurring on the nonpromoted PGM catalysts, there is a competitive adsorption on the same active sites between O$_2$, CO, and H$_2$. At low temperatures, the surface is covered predominantly with adsorbed CO, whereas O$_2$ and H$_2$ can be adsorbed on the surface at high temperatures only when the desorption of CO becomes obvious (Figure 3a). Therefore, the desorption of CO
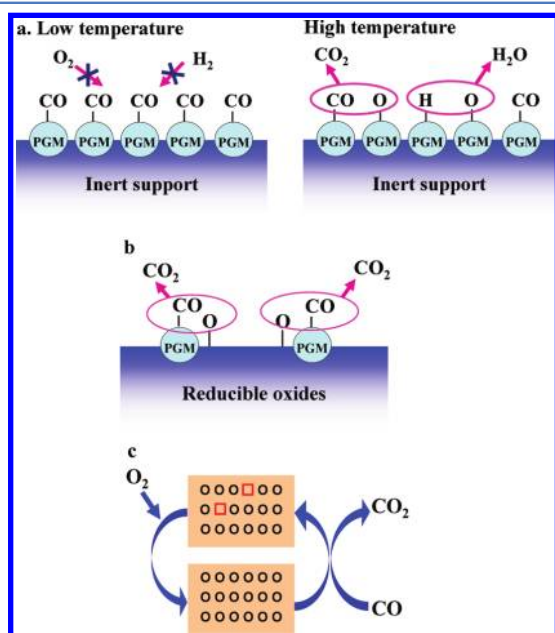

Figure 3. Different reaction pathways of PROX: (a) competitive Langmuir−Hinshelwood mechanism over nonpromoted PGM catalysts, (b) noncompetitive Langmuir−Hinshelwood mechanism over promoted PGM catalysts, and (c) Mars−van Krevelen mechanism over promoted PGM catalysts.

from the surface or the adsorption of O$_2$ is proposed as the rate-determining step on the nonpromoted PGM catalysts. As indicated in much of the literature,[19,164−166] the kinetics of the PROX reaction over Al$_2$O$_3$-supported noble metal catalysts can be expressed by a simple power-law rate equation:

$$r = A \exp(-E_a/RT)P_{CO}{}^{\alpha}P_{O_2}{}^{\beta}$$

where r is the reaction rate; A is the exponential factor; E_a is the activation energy; and α and β are the reaction orders for CO and O$_2$ pressures, respectively.

The apparent activation energy is found to be in the range of 70−100 kJ/mol at temperatures up to 200 °C, increasing at higher temperatures and CO partial pressures. The reaction orders are found to be negative for the CO partial pressure and positive for the oxygen partial pressure, respectively. These

kinetics are consistent with a Langmuir−Hinshelwood reaction mechanism in the *low-rate branch*,[165,167] on a surface predominantly covered with adsorbed CO. Such a competitive Langmuir−Hinshelwood reaction mechanism well predicts the low activity of noble metals at low temperatures owing to the inhibiting effect of CO adlayer on the O$_2$ adsorption. Increasing temperatures leads to the desorption of CO so that O$_2$ can be adsorbed and activated on the surface of noble metals.

Therefore, to reach the goal of removing CO in H$_2$, it is paramount to weaken the adsorption of CO on the surface of the noble metals. There are various approaches to make the CO adsorption weakened. For example, by changing the crystalline phase of γ-Al$_2$O$_3$ to α-Al$_2$O$_3$,[69] it was found that the adsorption of CO on Ru/α-Al$_2$O$_3$ was greatly weakened, which imparted to Ru/α-Al$_2$O$_3$ the highest activity for CO oxidation among the tested catalysts, especially at low temperatures, irrespective of the presence of H$_2$. It can reduce a high inlet concentration of CO to <10 ppm, even in the presence of H$_2$O and CO$_2$ over a wide temperature range. On the other hand, the strength of the CO adsorption is closely related to the particle sizes; it decreases with increasing the particle size, which results in the activity for CO oxidation being inversely proportional to the particle size of noble metals.[168−172] The particle size of the catalysts could be tuned by calcination temperature and duration. The activation energy for the CO oxidation reaction was observed to decrease with increasing particle size.[168] The reaction orders with respect to oxygen partial pressures increase with increasing particle size, indicating a higher dependence of the reaction kinetics on the oxygen partial pressure on larger particles. The CO adsorption can also be weakened by forming bimetallic catalysts.[173] DFT studies suggest that the relative differences in the catalytic activities for the various core−shell M@Pt (M = Ru, Rh, Ir, Pd, or Au) NPs originate partially from the relative availability of CO-free Pt surface sites on the M@Pt NPs, which are necessary for O$_2$ activation.[103,110] In addition, it was suggested that the presence of H$_2$ in the reactant gas mixture enhanced dramatically the PROX reaction rate on Pt/NaY and Pt/Al$_2$O$_3$ catalysts, which could be partially ascribed to the interaction between CO$_{ad}$ and H$_{ad}$ or the competitive adsorption between H$_2$ and CO that weakened the adsorption of CO on the surface of noble metals.[165,167,174]

4.2. The Mechanism of PROX on the Promoted PGM Catalysts.
For MO$_x$-promoted PGM catalysts, the widely accepted mechanism is the noncompetitive Langmuir−Hinshelwood mechanism in which CO adsorbed on the noble metal sites reacts with O provided by MO$_x$ at the interface of the noble metal and MO$_x$ (Figure 3b). In this mechanism, the adsorption and activation of O$_2$ is no longer a rate-determining step.[53,129,175] The kinetics of the PROX reaction over this kind of catalysts can also be expressed by the same power-law rate equation as shown in section 4.1. E_a was found to be comparatively smaller than that on the nonpromoted PGM catalysts, which was in the range of 5−44 kJ/mol.[129,155,156] The reaction order was found to be positive for CO partial pressures on IrFe catalyst,[155] implying that the poisonous effect of CO is eliminated by introducing promoters.

On the other hand, since the MO$_x$ is easily reduced at the reaction temperature with the aid of PGMs, the Mars−van Krevelen mechanism (also called the redox mechanism) was also proposed in which the surface lattice oxygen directly participates in the reaction for CO oxidation (Figure 3c);[145] for example, on Ir-in-CeO$_2$[145] catalyst in which the iridium particles embedded in the ceria matrix and interacting strongly

with the ceria support could weaken the surface Ce−O bonds and facilitate the formation of more reducible oxygen. In CO oxidation, the CO takes an oxygen atom from the ceria surface and creates an oxygen vacancy. The gas-phase oxygen will adsorb on the vacancies and be activated by the electron-rich environment created by the vacancies. The role of gas-phase oxygen is limited to the regeneration of reduced ceria sites. The activated O_2 reacts with CO to form a carbonate, which decomposes to release CO_2 and heal the oxygen vacancy; thus, a catalytic cycle from CO to CO_2 is completed without direct participation of noble metals for providing CO adsorption sites.

By applying temporal analysis of products reactor measurements from 80 to 400 °C, Behm's group investigated the CO oxidation over MO_x-supported gold catalysts in detail and proposed a gold-assisted Mars−van Krevelen mechanism.[176,177] In this mechanism, the surface lattice oxygen of the support can be removed and replenished with the aid of gold, and the active oxygen species for CO oxidation are the surface lattice oxygen at the perimeter of the gold NPs on the support. Although the evidence for the Mars−van Krevelen mechanism were provided for the MO_x-supported gold catalyst system, a similar mechanism may be applicable to MO_x-supported PGM catalysts, considering that PGM NPs resemble gold NPs in promoting the reduction of MO_x support at a significantly decreased temperature. Actually, we have recently found that FeO_x-supported Pt and Pd catalysts also followed the noble metal-assisted Mars−van Krevelen mechanism in the PROX reaction.

Nevertheless, it must be kept in mind that various types of mechanisms may work together for some catalyst systems, depending on the reaction temperature.[178] For example, four types of reaction mechanisms were suggested to be present simultanously for $Pt/CeZrO_x$ catalysts:[128] (i) a competitive Langmuir−Hinshelwood mechanism on the Pt particles; (ii) a noncompetitive Langmuir−Hinshelwood mechanism on the interface of Pt and $CeZrO_x$, which was predominant at 90−130 °C; (iii) a hydrogen oxidation on the $CeZrO_x$ support; and (iv) a water-gas-shift reaction at high temperatures.

The presence of MO_x not only provides reactive oxygen but also weakens the adsorption of CO on the noble metal sites due to the strong interaction between the noble metals and the MO_x.[175] For PtFe or IrFe catalysts, FTIR, TPR, and TPD data showed that CO coverage and CO bond strength on Pt or Ir were lowered significantly by the addition of FeO_x.[116,119,175,179] The FeO_x is proposed to be located on the surface of noble metal particles, blocking some of the noble metal surface and, consequently, decreasing the amount of CO adsorbed. In addition, the bridged CO is proposed to be more reactive than the linearly bonded CO with respect to O_2 on $FeO_x/Pt/TiO_2$.[180] According to FTIR results, the addition of alkali metals to a Pt single metal catalyst gave the bridge and 3-fold CO, thus weakened the adsorption of CO and enhanced the activity for CO oxidation.[160] Nevertheless, it cannot be concluded that "the weaker the CO adsorption is, the higher the activity or selectivity is". It was reported that the easier CO desorption from the niobia-promoted Pt catalyst resulted in lowering in the selectivity for CO oxidation, since the sites released by CO desorption accelerated the H_2 oxidation reaction.[132] For Rh/Nb_2O_5 catalyst, although the chemisorption ability toward CO changed drastically by the strong metal−support interactions induced by the calcination or reduction treatments, no direct correlation between the CO

chemisorption ability and the activity and selectivity has been found.[77,78]

When the reducible metal oxide is used as a promoter rather than as a support, it is usually highly dispersed together with the noble metal components on an inert support. HRTEM in combination with EDX reveals the noble metal is intimately contacting with the reducible metal oxide, which results in an enhanced interaction between them, thus giving a high activity for the PROX reaction.[119,179] For the alloy catalyst systems such as Pt−Fe, Pt−Co, Pt−Ni, and Pt−Sn, although the alloy phase is formed during the synthesis or the prereduction treatment of the catalyst, it will segregate into the intimately contacted noble metal and MO_x in the PROX reaction conditions,[141,181] as shown in Figure 2. For example, the formation of FeIr alloy was observed after the reduction in H_2, whereas the alloy phase was oxidized and segregated into Fe^{2+} and metallic Ir after the treatment in the PROX gas mixture.[154] A similar phenomenon was also observed for PtSn[181] and PtNi[139−142] catalysts. The entity PGM−MO_x which is derived from the PGM−M alloy, functions as the dual active sites where CO adsorbed on PGM reacts with the active oxygen provided by MO_x at the interface. The maximized interface due to the greatly reduced sizes of both PGM and MO_x and the strong interaction yielded by the alloy precursor are responsible for the enhanced activity for PROX;[141] however, the synergistic effect between PGM and M appears to be limited to the case of inert support. For the active support such as Nb_2O_5,[132] the addition of tin induces the Pt−Sn alloy formation, but the bimetallic interaction was partially suppressed by the niobia support while the Pt−Nb_2O_5 interaction was suppressed by the addition of Sn. In such a case, adding Sn has a negative effect on the activity of Pt/Nb_2O_5 catalyst.

In addition to the strong interaction between noble metals and reducible metal oxides, maintaining the reducible metal oxides at a low valence is also very important for keeping a high activity for CO oxidation because the low-valence metal oxides function as the sites for activating O_2. The presence of a large excess amount of H_2 in the PROX atmosphere plays a key role in maintaining the metal oxide at a low valence state. A commonly observed phenomenon in the PGM−MO_x catalyst systems is that the activity decreases with time on-stream in CO oxidation while it is stable in the PROX atmosphere.
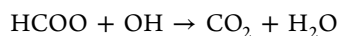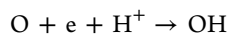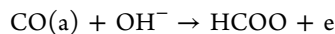
Isotopic transient kinetic analysis revealed that the reoxidation of Fe, instead of carbon accumulation, was responsible for the activity loss of PtFe catalyst in CO oxidation.[182] According to the XANES analysis,[55] Fe sites exist dominantly as FeO phase during the PROX reaction. We have used a combination of quasi in situ Mössbauer spectroscopy, in situ DRIFTS, and microcalorimetry to study systematically the oxidation state of Fe as a function of H_2 concentration for the PROX reaction over Ir−Fe catalysts.[154] The Fe^{3+} in the Ir−Fe/SiO_2 catalyst is easily reduced to low-valence Fe^{n+} (2 < n < 3), Fe^0, Fe^{2+}, and FeIr alloy with the aid of Ir, and the reduced Fe species are also easily oxidized upon exposure to oxygen.

Upon exposure to the PROX reaction gas mixture, the reduced catalyst turned into a real active catalyst that contained only three Fe species: Fe^{3+}, Fe^{2+}, and Fe^0. It was found that the promotional role of Fe was associated with the presence of H_2, and the relative amount of Fe^{2+} increased with increasing the H_2 concentration in the reaction stream.[154] This is very consistent with the trend of reaction rate for CO oxidation, strongly suggesting that Fe^{2+} was the active site for oxygen activation. On the other hand, about half the amount of Fe^0 in

the reduced Ir−Fe catalyst remained intact during the PROX reaction, implying that Fe^0 is probably encapsulated by iron oxide and does not play the part of activating O_2 in the PROX reaction. Moreover, by means of changing the deposition sequence of Ir and Fe, the amount of active Fe^{2+} species in the catalyst could be tuned, and consequently, the activity of the PROX reaction was altered. The IrFe catalyst prepared by coimpregnation contained more Fe^{2+} and gave a better performance for the PROX reaction.[153] The important role of Fe^{2+} is further confirmed by surface science and theoretical studies.[115] Similar to the low-valence FeO_x in Pt−Fe or Ir−Fe catalyst systems, SnO_x islands adjacent to the PtSn particles are also proposed as the active sites for O_2 activation.[129]
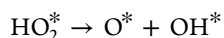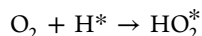
4.3. The Roles of the OH Group. The mechanism of PROX is often assumed as the competitive reaction of CO and H with O. In this assumption, the presence of H_2 will impose the only negative effect of decreasing the selectivity of CO oxidation. This is the actual case at high temperatures. However, the presence of H_2 is observed to have a remarkable enhancement for the low-temperature CO oxidation. Moreover, this effect is much more pronounced when a reducible oxide or an alkali promoter is present. Obviously, this promotional effect cannot be explained by the above competitive reaction mode. To give an insightful understanding of the effect of H_2 or H_2O, both the kinetic and theoretical calculations have been conducted, and various reaction mechanisms have been proposed accordingly.[183−186]

By investigating the dynamics of the intermediates for low-temperature PROX over $FeO_x/Pt/TiO_2$ and Pt/carbons with in situ DRIFT technique,[184−187] Tanaka et al. proposed that hydroxyl groups participate directly in the CO oxidation reaction through the following pathway:

$$CO(a) + OH^- \rightarrow HCOO + e$$

$$O + e + H^+ \rightarrow OH$$

$$HCOO + OH \rightarrow CO_2 + H_2O$$

In this mechanism, the reaction between the formate (HCOO) and hydroxyl groups is regarded as the rate-determining step.
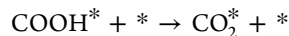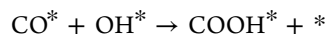
In the absence of hydroxyl groups on the support surface, the hydroxyl groups can be produced by the reaction between H_2 and O_2 via the following pathway:[188]

$$O_2 + H^* \rightarrow HO_2^*$$

$$HO_2^* \rightarrow O^* + OH^*$$

This route is also called H-assisted O_2 dissociation, which explains well the promotional effect of H_2 on the CO oxidation over Ru@Pt core−shell nanoparticles.[103,110]
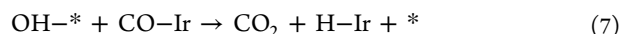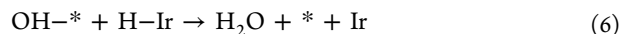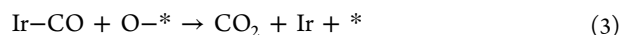
For some catalysts, the carboxyl (COOH) intermediates are proposed to play an important role in the PROX reaction. Microkinetic studies of CO oxidation, the water-gas shift reaction, and the PROX reaction on Pt and Rh catalysts reveal that the CO + O reaction in WGS and PROX reactions is slow, and additional CO−H_2 coupling reactions, including the carboxyl and hydroxyl intermediates as well as H_2O, are crucial steps for these processes.[189,190] Furthermore, CO−H_2 coupling via CO + OH reaction may involve a direct CO_2 formation as well as an indirect pathway via the formate or carboxyl intermediate for these catalysts.[189] The direct oxidation path dominates over the indirect path in the water-promoted CO

oxidation, whereas the indirect carboxyl path plays a vital role in the WGS and PROX simulations:[190]

$$CO^* + OH^* \rightarrow COOH^* + *$$

$$COOH^* + * \rightarrow CO_2^* + *$$

In this mechanism, the formate path was suggested to be unimportant for PROX,[189,190] Clearly, under these conditions, hydrogen acts as a "catalyst" for CO oxidation.

In some cases, the direct formation of CO_2 from CO and OH is the dominant pathway. Our group observed by IR spectroscopy that with the exception of CO, no other species, such as formyls or carbonates, are present on the surface of IrFe in the temperature range of 20−150 °C.[155] A similar phenomenon was also observed on PtSn.[130] On IrFe catalysts, a microkinetic model was established on the basis of the results of characterization and steady state kinetic data in a microreactor.[155] The elementary steps involved in the PROX reaction on the Ir−Fe catalyst can be described as eqs 1−7:

$$CO + Ir \leftrightarrows Ir-CO \tag{1}$$

$$O_2 + 2* \rightarrow 2O^* \tag{2}$$

$$Ir-CO + O-* \rightarrow CO_2 + Ir + * \tag{3}$$

$$H_2 + 2Ir \leftrightarrows 2H-Ir \tag{4}$$

$$H-Ir + O-* \leftrightarrows OH-* + Ir \tag{5}$$

$$OH-* + H-Ir \rightarrow H_2O + * + Ir \tag{6}$$

$$OH-* + CO-Ir \rightarrow CO_2 + H-Ir + * \tag{7}$$

where the asterisk, *, denotes a reduced iron site (Fe^{2+}). In the absence of H_2 (i.e., CO oxidation only), only steps 1−3 are involved in the reaction model. The model suggested that no competitive adsorption between CO and O_2 was observed for CO oxidation; both the adsorption of CO and O_2 reached saturation on Ir and Fe^{2+}, respectively, and the coverages of CO and O were irrelevant to the partial pressure of CO or O_2. The surface reaction between CO and O was the rate-determining step; however, for the PROX reaction, CO can be oxidized not only by atomic O, but also by the surface OH (step 7). The reaction between adsorbed H and O for the formation of OH (step 5) was rate-limiting for PROX, and the oxidation of adsorbed CO by surface OH (step 7) was the dominant pathway for PROX, rather than by atomic O. The fast increase in the coverage of OH on Fe^{2+} with the increase in the H_2 concentrations up to 10% coincides with the increase in the reaction rate of CO oxidation, indicating that OH plays an important role in the PROX reaction. The presence of H_2 increases the surface concentration of OH and, hence, lowers the activation energy and increases the reaction rate of PROX. Therefore, H_2 not only stabilizes Fe^{2+} species but also increases OH groups on the surface, both of which can promote CO oxidation. The reaction model of PROX on Ir−Fe catalyst is illustrated in Figure , where both steps 3 and 7 are considered.

It was suggested that the promotional role of alkali metals is also closely related to the increased concentration of OH groups neighboring to the noble metals. Very recently, Zhai et al.[191] used sub-ångström resolution aberration-corrected HAADF-STEM in combination with theoretical approaches to study the water-gas shift reaction over a Na-promoted Pt/SiO_2 catalyst. According to these observations, the promotional role of alkali metals can be understood in two aspects: one is to
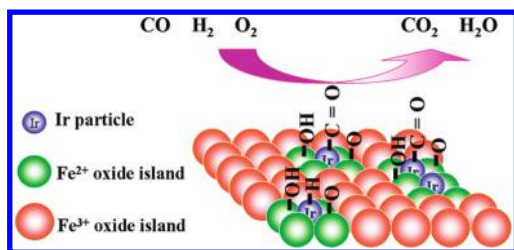
Figure 4. Schematic illustration of the PROX reaction over IrFe catalyst where the important roles of OH are considered.

stabilize the active Pt atoms, and the other is to provide the reactive OH species neighboring to the Pt atoms.

Our recent findings on the Pt single atom catalyst provided even more clear evidence for the roles of OH group in stabilizing Pt atom on iron oxide support.[116] By using a FeO_x support that is rich in OH groups and with a high surface area, the Pt metal can be well dispersed into single atoms on the surface of the FeO_x. Both experimental and theoretical studies show that Pt single atoms carry positive charges, and the remarkable catalytic activity of single Pt atoms in the PROX reaction is correlated with the partially vacant 5d orbitals of positively charged, high-valence Pt atoms, which help to reduce both the CO adsorption energy and the activation barriers for CO oxidation. Therefore, it appears that the active sites on the MO_x-promoted Pt catalysts are the same as those on the alkali metal-promoted Pt catalysts on inert supports. In the case of a reducible oxide as a promoter/support, the Pt single atoms can be stabilized with the OH groups on the MO_x, and the OH groups neighboring the Pt atoms are reactive toward CO to produce CO_2.

Different from the explanation by enhancement of OH groups, Iglesia and co-workers proposed that alkali metals promoted the catalytic activity of Pt/Al_2O_3 (or Pt/SiO_2) for the PROX reaction mainly via the inhibition of the spillover-mediated H_2 oxidation pathway and of growth of dense chemisorbed CO islands on the surface of Pt clusters;[160] however, the coupling effect between H_2 and CO was not considered in their work.

In the above examples, the OH groups are associated with the presence of promoters, either on the reducible oxide support or on the alkali metal-promoted Al_2O_3 or SiO_2 surfaces. Quite different from these examples, Fukuoka's group found that Pt nanoparticles supported on FSM-type mesoporous silica were extremely active and selective for the PROX of CO; both the CO conversion and the CO_2 selectivity were above 95% at 25−150 °C over Pt/FSM-16.[192] By using an isotopic tracer technique in combination with the IR experiments, the authors came to the conclusion that the OH groups at the internal surface of mesoporous silica are reactive toward CO to produce CO_2. Such an unprecedented reactivity of OH groups on the silica surface appears to be closely related with the pore structure and pore size.[192] Since only a very limited number of mesoporous silica possess such highly reactive OH groups, a more rational correlation between the reactivity of OH groups and the silica structure need to be established.

The important roles of OH groups are also demonstrated in the effect of water. It is commonly observed that the addition of water to the reaction stream[157,180,184−186] or the pretreatment of catalyst with water vapor[6] can lead to a large increase in the activity for a low-temperature PROX reaction. Such enhancement was proposed to be due in part to the formation of

oxidant hydroxyl groups on the catalyst surface because no evident WGS reaction was detected on most of the noble metal catalyst systems at relatively low reaction temperatures.

5. SUMMARY AND REMARKS

The supported transition metals are a kind of attractive candidate as catalysts for the PROX reaction. Usually, the unpromoted transition metal catalysts show poor activities in the low temperature range (<120 °C), since the metal surface is predominantly covered with CO, which inhibits the adsorption of O_2. To enhance the low-temperature PROX activity of the transition metals, weakening the CO adsorption on the metal sites or providing vacant sites for O_2 adsorption/activation (or both) are the prerequisites. Following this rule, the catalytic performances of transiton metal catalysts can be improved greatly by the employment of the following three types of promoters:

(i) *Reducible oxides.* The transition metals in combination with reducible oxides, either as the supports or just as a minor amount of promoters, show high activities and selectivities for the PROX reaction in the low temperature range, which is quite different from the unpromoted counterparts. There are at least two important roles of the reducible oxides: one is to weaken the CO adsorption on the transition metal sites and the other is to provide additional sites for adsorption/activation of O_2, thus changing the competitive L−H mechanism into a noncompetitive dual site L−H mechanism. Among various reducible oxides, iron oxide (FeO_x) appears to be the most remarkable one; the Pt−Fe catalyst shows the most promising catalytic performance in the real PROX operation conditions.

(ii) *Alkali metal cations.* The addition of alkali or alkali earth metal cations to the transition metal catalysts brings about up to a 10-fold enhancement in the low-temperature PROX activity. Similar to the reducible oxides, the addition of alkali metal cations can also weaken the adsorption of CO on the transition metals. However, a more underlying reason for the promotional effect is that the alkali cations provide reactive OH groups neighboring the transition metals such as Pt. These OH groups react smoothly with CO adsorbed on neighboring Pt atoms to give CO_2 as the product. Actually, the important roles of surface OH groups in the PROX reaction are being accepted by more and more researchers, especially with the aid of theoretical calculations.

(iii) *The second transition metal component.* Introduction of the second transition metal component to form a bimetallic nanostructure is another useful approach to weaken the CO adsorption. Depending on the miscibility and surface free energy of the two metals, different bimetallic nanostructures, such as core−shell and alloy, can be obtained just by variation in the deposition sequence of the two metals or changing the pretreatment temperature and atmosphere. A typical example is Ru@Pt core−shell nanocatalyst which shows a weakened interaction with CO and thus an enhanced low-temperature activity for PROX. One advantage of such bimetallic structure is its controllable size, morphology, composition, and structure, which endows it a good model catalyst system for studying the structure-performance relationship.

Although the above three types of promoters have been proved effective, the approaches for the enhancement of PROX activities of transition metal catalysts are absolutely not limited to them. In particular, by increasing the surface OH groups and making them more reactive toward CO, for example, by using a metal hydroxide rather than oxide as the support,[155] or by using a mesoporous silica support that possesses confined space with rich internal OH groups,[192,193] one can also achieve a greatly improved performance for PROX. Even with the same promoter, different preparation methods and pretreatment conditions will lead to a quite different performances of the final catalysts. It can be expected that with the advancement of materials science, new catalysts with the desired activity, selectivity, and durability for the PROX reaction will be developed in the future.

On the other hand, the evaluation of a PROX catalyst requires the testing of the catalytic performance in a simulated reformate gas atmosphere, that is, a significant amount of CO_2 and steam is contained in the feedstock, which is ignored by most laboratory studies. Some highly active catalysts in an ideal feed gas condition may seriously lose their activities when exposed to a high concentration of CO_2 and H_2O. In addition, very few papers have focused on the lifetime of the catalysts during the PROX reaction, especially in reformate gas mixtures. Therefore, when a new catalyst is developed for the PROX process, the evaluation of its lifetime under simulated conditions should be strongly encouraged.

In fundamental science, a great deal of attention has been put on the clarification of the reaction mechanism over the promoted transition metal catalysts. In particular, with the advancement of in situ characterization techniques, of atomic-resolution electron microscopy techniques and of theoretical calculations on more complex systems, the identification of active sites is now becoming possible. Some excellent contributions in this respect have emerged recently.[115,116,194] Future efforts in this area should be encouraged with the aim of revealing the nature of the active oxygen provided by reducible oxide, the identification of real active sites that are possibly composed of a transition metal and neighboring OH groups, and the understanding of the respective role of transition metals and promoters. Moreover, the promoted transition metal catalysts are reminiscent of gold nanocatalysts in the PROX reactions. Accordingly, a comparative study that will give a better understanding of the nature of catalysis should be encouraged.

■ AUTHOR INFORMATION

Corresponding Author
*Phone: 86-411-84379015. Fax: 86-411-84691570. E-mail: taozhang@dicp.ac.cn.

Present Address
†Research Center for Eco-Environmental Sciences, Chinese Academy of Sciences, Beijing 100085, P. R. China

Notes
The authors declare no competing financial interest.

■ ACKNOWLEDGMENTS

■ REFERENCES

(1) Wu, J. F.; Yuan, X. Z.; Martin, J. J.; Wang, H. J.; Zhang, J. J.; Shen, J.; Wu, S. H.; Merida, W. *J. Power Sources* **2008**, *184*, 104−119.
(2) O'Connell, M.; Kolb, G.; Schelhaas, K.; Schuerer, J.; Tiemann, D.; Ziogas, A.; Hessel, V. *Int. J. Hydrogen Energy* **2010**, *35*, 2317−2327.
(3) Trimm, D. L. *Appl. Catal., A* **2005**, *296*, 1−11.
(4) Si, R.; Flytzani-Stephanopoulos, M. *Angew. Chem.* **2008**, *120*, 2926−2929.
(5) Ghenciu, A. F. *Curr. Opin. Solid State Mater. Sci.* **2002**, *6*, 389−399.
(6) Son, I. H.; Shamsuzzoha, M.; Lane, A. M. *J. Catal.* **2002**, *210*, 460−465.
(7) Jiménez, S.; Soler, J.; Valenzuela, R. X.; Daza, L. *J. Power Sources* **2005**, *151*, 69−73.
(8) Lemons, R. A. *J. Power Sources* **1990**, *29*, 251−264.
(9) Tosti, S. *Int. J. Hydrogen Energy* **2010**, *35*, 12650−12659.
(10) Liu, Q. H.; Liao, L. W.; Zhou, X. H.; Yin, G. Q. *Adv. Mater. Res.* **2011**, *236−238*, 829−834.
(11) Park, E. D.; Lee, D.; Lee, H. C. *Catal. Today* **2009**, *139*, 280−290.
(12) Choudhary, T. V.; Goodman, D. W. *Catal. Today* **2002**, *77*, 65−78.
(13) Thomas, C. E.; James, B. D.; Lomax, F. D.; Kuhn, I. F. *Int. J. Hydrogen Energy* **2000**, *25*, 551−567.
(14) Cohn, J. G. E. U.S. Patent 3216782, 1965.
(15) Okumura, M.; Masuyama, N.; Konishi, E.; Ichikawa, S.; Akita, T. *J. Catal.* **2002**, *208*, 485−489.
(16) Li, B. D.; Wang, C.; Yi, G. Q.; Lin, H. Q.; Yuan, Y. Z. *Catal. Today* **2011**, *164*, 74−79.
(17) Kipnis, M.; Volnina, E. *Appl. Catal., B* **2010**, *98*, 193−203.
(18) Oh, S. H.; Sinkevitch, R. M. *J. Catal.* **1993**, *142*, 254−262.
(19) Kim, D. H.; Lim, M. S. *Appl. Catal., A* **2002**, *224*, 27−38.
(20) Scirè, S.; Riccobene, P. M.; Crisafulli, C. *Appl. Catal., B* **2010**, *101*, 109−117.
(21) Avgouropoulos, G.; Papavasiliou, J.; Tabakova, T.; Idakiev, V.; Ioannides, T. *Chem. Eng. J.* **2006**, *124*, 41−45.
(22) Laguna, O. H.; Sarria, F. R.; Centeno, M. A.; Odriozola, J. A. *J. Catal.* **2010**, *276*, 360−370.
(23) Tu, C. H.; Wang, A. Q.; Zheng, M. Y.; Meng, Y.; Shan, J. H.; Zhang, T. *Chin. J. Catal.* **2005**, *26*, 631−633.
(24) Tu, C. H.; Wang, A. Q.; Zheng, M. Y.; Wang, X. D.; Zhang, T. *Appl. Catal., A* **2006**, *297*, 40−47.
(25) Schubert, M. M.; Hackenberg, S.; van Veen, A. C.; Muhler, M.; Plzak, V.; Behm, R. J. *J. Catal.* **2001**, *197*, 113−122.
(26) Haruta, M.; Kobayashi, T.; Sano, H.; Yamada, N. *Chem. Lett.* **1987**, 405−408.
(27) Bond, G.; Thompson, D. *Gold Bull.* **2009**, *42*, 247−259.
(28) Lippits, M. J.; Gluhoi, A. C.; Nieuwenhuys, B. E. *Top. Catal.* **2007**, *44*, 159−165.
(29) Liu, Y.; Jia, C.-J.; Yamasaki, J.; Terasaki, O.; Schüth, F. *Angew. Chem., Int. Ed.* **2010**, *49*, 5771−5775.
(30) Zhao, K. F.; Qiao, B. T.; Wang, J.; Zhang, Y. J.; Zhang, T. *Chem. Commun.* **2011**, 1779−1781.
(31) Qiao, B. T.; Wang, A. Q.; Takahashi, M.; Zhang, Y. J.; Wang, J.; Deng, Y. Q.; Zhang, T. *J. Catal.* **2011**, *279*, 361−365.
(32) Lin, C.-H.; Liu, X. Y.; Wu, S.-H.; Liu, K.-H.; Mou, C.-Y. *J. Phys. Chem. Lett.* **2011**, *2*, 2984−2988.
(33) Piccolo, L.; Daly, H.; Valcarel, A.; Meunier, F. C. *Appl. Catal., B* **2009**, *86*, 190−195.
(34) Denkwitz, Y.; Schumacher, B.; Kučerová, G.; Behm, R. J. *J. Catal.* **2009**, *267*, 78−88.
(35) Oh, H.-S.; Yang, J. H.; Costello, C. K.; Wang, Y. M.; Bare, S. R.; Kung, H. H.; Kung, M. C. *J. Catal.* **2002**, *210*, 375−386.
(36) Carrettin, S.; Concepción, P.; Corma, A.; López-Nieto, J. M.; Puntes, V. F. *Angew. Chem., Int. Ed.* **2004**, *43*, 2538−2540.
(37) Quinet, E.; Piccolo, L.; Morfin, F.; Avenier, P.; Diehl, F.; Caps, V.; Rousset, J. *J. Catal.* **2009**, *268*, 384−389.
(38) Wang, H.; Zhu, H. Q.; Qin, Z. F.; Liang, F. X.; Wang, G. F.; Wang, J. G. *J. Catal.* **2009**, *264*, 154−162.

(39) Galletti, C.; Fiorot, S.; Specchia, S.; Saracco, G.; Specchia, V. *Chem. Eng. J.* **2007**, *134*, 45−50.

(40) Xu, J.; Li, P.; Song, X. F.; Qi, Z. W.; Yu, J. G.; Yuan, W. K.; Han, Y.-F. *Ind. Eng. Chem. Res.* **2010**, *49*, 4149−4155.

(41) Park, J. W.; Jeong, J. H.; Yoon, W. L.; Kim, C. S.; Lee, D.-K.; Park, Y.-K.; Rhee, Y. W. *Int. J. Hydrogen Energy* **2005**, *30*, 209−220.

(42) Razeghi, A.; Khodadadi, A.; Ziaei-Azad, H.; Mortazavi, Y. *Chem. Eng. J.* **2010**, *164*, 214−220.

(43) Mariño, F.; Baronetti, G.; Laborde, M.; Bion, N.; Le Valant, A.; Epron, F.; Duprez, D. *Int. J. Hydrogen Energy* **2008**, *33*, 1345−1353.

(44) Kydd, R.; Ferri, D.; Hug, P.; Scott, J.; Teoh, W. Y.; Amal, R. *J. Catal.* **2011**, *277*, 64−71.

(45) Maciel, C. G.; Profeti, L. P. R.; Assaf, E. M.; Assaf, J. M. *J. Power Sources* **2011**, *196*, 747−753.

(46) Hornés, A.; Hungría, A. B.; Bera, P.; López Cámara, A.; Fernández-García, M.; Martínez-Arias, A.; Barrio, L.; Estrella, M.; Zhou, G.; Fonseca, J. J.; Hanson, J. C.; Rodriguez, J. A. *J. Am. Chem. Soc.* **2010**, *132*, 34−35.

(47) Caputo, T.; Lisi, L.; Pirone, R.; Russo, G. *Appl. Catal., A* **2008**, *348*, 42−53.

(48) Sirichaiprasert, K.; Luengnaruemitchai, A.; Pongstabodee, S. *Int. J. Hydrogen Energy* **2007**, *32*, 915−926.

(49) Zou, H. B.; Chen, S. Z.; Liu, Z. L.; Lin, W. M. *Int. J. Hydrogen Energy* **2009**, *34*, 9324−9333.

(50) Qiao, B. T.; Wang, A. Q.; Lin, J.; Li, L.; Su, D. S.; Zhang, T. *Appl. Catal., B* **2011**, *105*, 103−110.

(51) Korotkikh, O.; Farrauto, R. *Catal. Today* **2000**, *62*, 249−254.

(52) Watanabe, M.; Uchida, H.; Ohkubo, K.; Igarashi, H. *Appl. Catal., B* **2003**, *46*, 595−600.

(53) Kotobuki, M.; Watanabe, A.; Uchida, H.; Yamashita, H.; Watanabe, M. *J. Catal.* **2005**, *236*, 262−269.

(54) Kotobuki, M.; Watanabe, A.; Uchida, H.; Yamashita, H.; Watanabe, M. *Appl. Catal., A* **2006**, *307*, 275−283.

(55) Kotobuki, M.; Shido, T.; Tada, M.; Uchida, H.; Yamashita, H.; Iwasawa, Y.; Watanabe, M. *Catal. Lett.* **2005**, *103*, 263−269.

(56) Manasilp, A.; Gulari, E. *Appl. Catal., B* **2002**, *37*, 17−25.

(57) Zhou, S. L.; Yuan, Z. S.; Wang, S. D. *Int. J. Hydrogen Energy* **2006**, *31*, 924−933.

(58) Snytnikov, P. V.; Sobyanin, V. A.; Belyaev, V. D.; Tsyrulnikov, P. G.; Shitova, N. B.; Shlyapin, D. A. *Appl. Catal., A* **2003**, *239*, 149−156.

(59) Alexeev, O. S.; Chin, S. Y.; Engelhard, M. H.; Ortiz-Soto, L.; Amiridis, M. D. *J. Phys. Chem. B* **2005**, *109*, 23430−23433.

(60) Chin, S. Y.; Alexeev, O. S.; Amiridis, M. D. *Appl. Catal., A* **2005**, *286*, 157−166.

(61) Echigo, M.; Tabata, T. *Top. Catal* **2009**, *52*, 739−742.

(62) Echigo, M.; Tabata, T. *Appl. Catal., A* **2003**, *251*, 157−166.

(63) Echigo, M.; Tabata, T. *Catal. Lett.* **2004**, *98*, 37−42.

(64) Echigo, M.; Tabata, T. *Catal. Today* **2004**, *90*, 269−275.

(65) Echigo, M.; Shinke, N.; Takami, S.; Tabata, T. *J. Power Sources* **2004**, *132*, 29−35.

(66) Echigo, M.; Shinke, N.; Takami, S.; Higashiguchi, S.; Hirai, K.; Tabata, T. *Catal. Today* **2003**, *84*, 209−215.

(67) Echigo, M.; Tabata, T. *J. Chem. Eng. Jpn.* **2004**, *37*, 558−562.

(68) Rosso, I.; Antonini, M.; Galletti, C.; Saracco, G.; Specchia, V. *Top. Catal.* **2004**, *30−31*, 475−480.

(69) Kim, Y. H.; Park, E. D. *Appl. Catal., B* **2010**, *96*, 41−50.

(70) Kim, Y. H.; Park, E. D.; Lee, H. C.; Lee, D. *Appl. Catal., A* **2009**, *366*, 363−369.

(71) Kim, Y. H.; Park, E. D.; Lee, H. C.; Lee, D.; Lee, K. H. *Catal. Today* **2009**, *146*, 253−259.

(72) Han, Y.-F.; Kinne, M.; Behm, R. J. *Appl. Catal., B* **2004**, *52*, 123−134.

(73) Xu, G. W.; Zhang, Z.-G. *J. Power Sources* **2006**, *157*, 64−77.

(74) Galletti, C.; Specchia, S.; Saracco, G.; Specchia, V. *Ind. Eng. Chem. Res.* **2008**, *47*, 5304−5312.

(75) Galletti, C.; Fiorot, S.; Specchia, S.; Saracco, G.; Specchia, V. *Top. Catal* **2007**, *45*, 15−19.

(76) Specchia, S.; Galletti, C.; Fiorot, S.; Saracco, G.; Specchia, V. *ECS Trans.* **2007**, *5*, 677−685.

(77) Ito, S.-I.; Fujimori, T.; Nagashima, K.; Yuzaki, K.; Kunimori, K. *Catal. Today* **2000**, *57*, 247−254.

(78) Ito, S.-I.; Tanaka, H.; Minemura, Y.; Kameoka, S.; Tomishige, K.; Kunimori, K. *Appl. Catal., A* **2004**, *273*, 295−302.

(79) Han, Y.-F.; Kahlich, M.; Kinne, M.; Behm, R. J. *Appl. Catal., B* **2004**, *50*, 209−218.

(80) Ren, S.; Hong, X. *Fuel Process. Technol.* **2007**, *88*, 383−386.

(81) Avgouropoulos, G.; Ioannides, T.; Papadopoulou, Ch.; Batista, J.; Hocevar, S.; Matralis, H. *Catal. Today* **2002**, *75*, 157−167.

(82) Watanabe, M.; Uchida, H.; Igarashi, H.; Suzuki, M. *Chem. Lett.* **1995**, *24*, 21−23.

(83) Kotobuki, M.; Watanabe, A.; Uchida, H.; Yamashita, H.; Watanabe, M. *Chem. Lett.* **2005**, 866−867.

(84) Igarashi, H.; Uchida, H.; Suzuki, M.; Sasaki, Y.; Watanabe, M. *Appl. Catal., A* **1997**, *159*, 159−169.

(85) Andorf, R.; Maunz, W.; Plog, C.; Stengel, T. U.S. Patent 5955395, 1999.

(86) Sebastian, V.; Irusta, S.; Mallada, R.; Santamaría, J. *Appl. Catal., A* **2009**, *366*, 242−251.

(87) Rosso, I.; Galletti, C.; Saracco, G.; Garrone, E.; Specchia, V. *Appl. Catal., B* **2004**, *48*, 195−203.

(88) Rosso, I.; Galletti, C.; Fiorot, S.; Saracco, G.; Garrone, E.; Specchia, V. *J. Porous Mater.* **2007**, *14*, 245−250.

(89) Galletti, C.; Specchia, S.; Saracco, G.; Specchia, V. *Chem. Eng. J.* **2009**, *154*, 246−250.

(90) Galletti, C.; Specchia, S.; Saracco, G.; Specchia, V. *Int. J. Hydrogen Energy* **2008**, *33*, 3045−3048.

(91) Wang, A. Q.; Liu, J.-H.; Lin, S. D.; Lin, T.-S.; Mou, C.-Y. *J. Catal.* **2005**, *233*, 186−197.

(92) Wang, A. Q.; Chang, C.-M.; Mou, C.-Y. *J. Phys. Chem. B* **2005**, *109*, 18860−18867.

(93) Wang, A. Q.; Hsieh, Y.-P.; Chen, Y.-F.; Mou, C.-Y. *J. Catal.* **2006**, *237*, 197−206.

(94) Liu, X. Y.; Wang, A. Q.; Wang, X. D.; Mou, C.-Y.; Zhang, T. *Chem. Commun.* **2008**, 3187−3189.

(95) Liu, X. Y.; Wang, A. Q.; Yang, X. F.; Zhang, T.; Mou, C.-Y.; Su, D.-S.; Li, J. *Chem. Mater.* **2009**, *21*, 410−418.

(96) Liu, X. Y.; Wang, A. Q.; Zhang, T.; Su, D.-S.; Mou, C.-Y. *Catal. Today* **2011**, *160*, 103−108.

(97) Liu, X. Y.; Wang, A. Q.; Li, L.; Zhang, T.; Mou, C.-Y.; Lee, J.-F. *J. Catal.* **2011**, *278*, 288−296.

(98) Srnová-Šloufová, I.; Vlčková, B.; Bastl, Z.; Hasslett, T. L. *Langmuir* **2004**, *20*, 3407−3415.

(99) Yin, A.-X.; Min, X.-Q.; Zhang, Y.-W.; Yan, C.-H. *J. Am. Chem. Soc.* **2011**, *133*, 3816−3819.

(100) Tao, A. R.; Habas, S.; Yang, P. D. *Small* **2008**, *4*, 310−325.

(101) Xia, Y. N.; Xiong, Y. J.; Lim, B.; Skrabalak, S. E. *Angew. Chem., Int. Ed.* **2008**, *47*, 2−46.

(102) Chen, J. Y.; Lim, B.; Lee, E. P.; Xia, Y. N. *Nano Today* **2009**, *4*, 81−95.

(103) Alayoglu, S.; Nilekar, A. U.; Mavrikakis, M.; Eichhorn, B. *Nat. Mater.* **2008**, *7*, 333−338.

(104) Yang, X. F.; Wang, Y. L.; Zhao, Y. F.; Wang, A. Q.; Zhang, T.; Li, J. *Phys. Chem. Chem. Phys.* **2010**, *12*, 3038−3043.

(105) Lee, S. H.; Han, J.; Lee, K.-W. *Korean J. Chem. Eng.* **2002**, *19*, 431−433.

(106) Chin, S. Y.; Alexeev, O. S.; Amiridis, M. D. *J. Catal.* **2006**, *243*, 329−339.

(107) Igarashi, H.; Uchida, H.; Watanabe, M. *Chem. Lett.* **2000**, 1262−1263.

(108) Naknam, P.; Luengnaruemitchai, A.; Wongkasemjit, S.; Osuwan, S. *J. Power Sources* **2007**, *165*, 353−358.

(109) Parinyaswan, A.; Pongstabodee, S.; Luengnaruemitchai, A. *Int. J. Hydrogen Energy* **2006**, *31*, 1942−1949.

(110) Nilekar, A. U.; Alayoglu, S.; Eichhorn, B.; Mavrikakis, M. *J. Am. Chem. Soc.* **2010**, *132*, 7418−7428.

(111) Maeda, N.; Matsushima, T.; Uchida, H.; Yamashita, H.; Watanabe, M. *Appl. Catal., A* **2008**, *341*, 93−97.

(112) Roberts, G. W.; Chin, P.; Sun, X. L.; Spivey, J. J. *Appl. Catal., B* **2003**, *46*, 601−611.

(113) Chin, P.; Sun, X. L.; Roberts, G. W.; Spivey, J. J. *Appl. Catal., A* **2006**, *302*, 22−31.

(114) Sirijiaruphan, A.; Goodwin, J. G., Jr.; Rice, R. W.; Wei, D. G.; Butcher, K. R.; Roberts, G. W.; Spivey, J. J. *Appl. Catal., A* **2005**, *281*, 11−18.

(115) Fu, Q.; Li, W. X.; Yao, Y. X.; Liu, H. Y.; Su, H.-Y.; Ma, D.; Gu, X.-K.; Chen, L. M.; Wang, Z.; Zhang, H.; Wang, B.; Bao, X. H. *Science* **2010**, *328*, 1141−1144.

(116) Qiao, B. T.; Wang, A. Q.; Yang, X. F.; Allard, L. F.; Jiang, Z.; Cui, Y. T.; Liu, J. Y.; Li, J.; Zhang, T. *Nat. Chem.* **2011**, *3*, 634−641.

(117) Tang, X. L.; Zhang, B. C.; Li, Y.; Xin, Q.; Shen, W. J. *Chin. J. Catal.* **2005**, *26*, 1−3.

(118) Yin, J.; Wang, J.; Zhang, T.; Wang, X. D. *Catal. Lett.* **2008**, *125*, 76−82.

(119) Siani, A.; Captain, B.; Alexeev, O. S.; Stafyla, E.; Hungria, A. B.; Midgley, P. A.; Thomas, J. M.; Adams, R. D.; Amiridis, M. D. *Langmuir* **2006**, *22*, 5160−5167.

(120) Mariño, F.; Descorme, C.; Duprez, D. *Appl. Catal., B* **2004**, *54*, 59−66.

(121) Pozdnyakova, O.; Teschner, D.; Wootsch, A.; Kröhnert, J.; Steinhauer, B.; Sauer, H.; Toth, L.; Jentoft, F. C.; Knop-Gericke, A.; Paál, Z.; Schlögl, R. *J. Catal.* **2006**, *237*, 1−16.

(122) Pozdnyakova-Tellinger, O.; Teschner, D.; Kröhnert, J.; Jentoft, F. C.; Knop-Gericke, A.; Schlögl, R.; Wootsch, A. *J. Phys. Chem. C* **2007**, *111*, 5426−5431.

(123) Ayastuy, J. L.; Gil-Rodríguez, A.; González-Marcos, M. P.; Gutiérrez-Ortiz, M. A. *Int. J. Hydrogen Energy* **2006**, *31*, 2231−2242.

(124) Teschner, D.; Wootsch, A.; Pozdnyakova-Tellinger, O.; Kröhnert, J.; Vass, E. M.; Hävecker, M.; Zafeiratos, S.; Schnörch, P.; Jentoft, P. C.; Knop-Gericke, A.; Schlögl, R. *J. Catal.* **2007**, *249*, 318−327.

(125) Teschner, D.; Wootsch, A.; Pozdnyakova, O.; Sauer, H.; Knop-Gericke, A.; Schlögl, R. *React. Kinet. Catal. Lett.* **2006**, *87*, 235−247.

(126) Roh, H.-S.; Potdar, H. S.; Jun, K.-W.; Han, S. Y.; Kim, J.-W. *Catal. Lett.* **2004**, *93*, 203−207.

(127) Ayastuy, J. L.; González-Marcos, M. P.; Gil-Rodríguez, A.; González-Velasco, J. R.; Gutiérrez-Ortiz, M. A. *Catal. Today* **2006**, *116*, 391−399.

(128) Wootsch, A.; Descorme, C.; Duprez, D. *J. Catal.* **2004**, *225*, 259−266.

(129) Schubert, M. M.; Kahlich, M. J.; Feldmeyer, G.; Hüttner, M.; Hackenberg, S.; Gasteiger, H. A.; Behm, R. *J. Phys. Chem. Chem. Phys.* **2001**, *3*, 1123−1131.

(130) Dupont, C.; Delbecq, F.; Loffreda, D.; Jugnet, Y. *J. Catal.* **2011**, *278*, 339−245.

(131) Dupont, C.; Jugnet, Y.; Loffreda, D. *J. Am. Chem. Soc.* **2006**, *128*, 9129−9136.

(132) Marques, P.; Ribeiro, N. F. P.; Schmal, M.; Aranda, D. A. G.; Souza, M. M. V. M *J. Power Sources* **2006**, *158*, 504−508.

(133) Özkara, S.; Aksoylu, A. E. *Appl. Catal., A* **2003**, *251*, 75−83.

(134) Caglayan, B. S.; Soykal, İ. I.; Aksoylu, A. E. *Appl. Catal., B* **2011**, *106*, 540−549.

(135) Komatsu, T.; Tamura, A. *J. Catal.* **2008**, *258*, 306−314.

(136) Epling, W. S.; Cheekatamarla, P. K.; Lane, A. M. *Chem. Eng. J.* **2003**, *93*, 61−68.

(137) Snytnikov, P. V.; Yusenko, K. V.; Korenev, S. V.; Shubin, Y. V.; Sobyanin, V. A. *Kinet. Catal.* **2007**, *48*, 276−281.

(138) Ko, E. Y.; Park, E. D.; Lee, H. C.; Lee, D.; Kim, S. *Angew. Chem., Int. Ed.* **2007**, *46*, 734−737.

(139) Ko, E.-Y.; Park, E. D.; Seo, K. W.; Lee, H. C.; Kim, S. *Catal. Lett.* **2006**, *110*, 275−279.

(140) Suh, D. J.; Kwak, C.; Kim, J.-H.; Kwon, S. M.; Park, T.-J. *J. Power Sources* **2005**, *142*, 70−74.

(141) Lu, S. H.; Zhang, C.; Liu, Y. *Int. J. Hydrogen Energy* **2011**, *36*, 1939−1948.

(142) Mu, R. T.; Fu, Q.; Xu, H.; Zhang, H.; Huang, Y. Y.; Jiang, Z.; Zhang, S.; Tan, D. L.; Bao, X. H. *J. Am. Chem. Soc.* **2011**, *133*, 1978−1986.

(143) Huang, Y. Q.; Wang, A. Q.; Wang, X. D.; Zhang, T. *Int. J. Hydrogen Energy* **2007**, *32*, 3880−3886.

(144) Huang, Y. Q.; Wang, A. Q.; Li, L.; Wang, X. D.; Zhang, T. *Catal. Commun.* **2010**, *11*, 1090−1093.

(145) Huang, Y. Q.; Wang, A. Q.; Li, L.; Wang, X. D.; Su, D. S.; Zhang, T. *J. Catal.* **2008**, *255*, 144−152.

(146) Lin, J.; Huang, Y. Q.; Li, L.; Qiao, B. T.; Wang, X. D.; Wang, A. Q.; Zhang, T. *Chem. Eng. J.* **2011**, *168*, 822−826.

(147) Lin, J.; Li, L.; Wang, X. D.; Huang, Y. Q.; Wang, A. Q.; Zhang, T. *Sci. China Ser. B: Chem.* **2010**, *40*, 1409−1414.

(148) Lin, J.; Li, L.; Huang, Y. Q.; Zhang, W. S.; Wang, X. D.; Wang, A. Q.; Zhang, T. *J. Phys. Chem. C* **2011**, *115*, 16509−16517.

(149) Lin, J.; Huang, Y. Q.; Li, L.; Wang, A. Q.; Zhang, W. S.; Wang, X. D.; Zhang, T. *Catal. Today* **2012**, *180*, 155−160.

(150) Zhang, W. S.; Wang, A. Q.; Li, L.; Wang, X. D.; Zhang, T. *Catal. Lett.* **2008**, *121*, 319−323.

(151) Zhang, W. S.; Wang, A. Q.; Li, L.; Wang, X. D.; Zhang, T. *Catal. Today* **2008**, *131*, 457−463.

(152) Zhang, W. S.; Huang, Y. Q.; Wang, J.; Liu, K.; Wang, X. D.; Wang, A. Q.; Zhang, T. *Int. J. Hydrogen Energy* **2010**, *35*, 3065−3071.

(153) Liu, K.; Wang, A. Q.; Zhang, W. S.; Wang, J.; Huang, Y. Q.; Jin, C. Z.; Shen, J. Y.; Zhang, T. *Chin. J. Catal.* **2010**, *31*, 1335−1341.

(154) Liu, K.; Wang, A. Q.; Zhang, W. S.; Wang, J.; Huang, Y. Q.; Shen, J. Y.; Zhang, T. *J. Phys. Chem. C* **2010**, *114*, 8533−8541.

(155) Liu, K.; Wang, A. Q.; Zhang, W. S.; Wang, J.; Huang, Y. Q.; Wang, X. D.; Shen, J. Y.; Zhang, T. *Ind. Eng. Chem. Res.* **2011**, *50*, 758−766.

(156) Lin, J.; Qiao, B. T.; Liu, J. Y.; Huang, Y. Q.; Wang, A. Q.; Li, L.; Zhang, W. S.; Allard, L. F.; Wang, X. D.; Zhang, T. *Angew. Chem., Int. Ed.*; DOI: 10.1002/anie.201106702.

(157) Cho, S.-H.; Park, J.-S.; Choi, S.-H.; Kim, S.-H. *J. Power Sources* **2006**, *156*, 260−266.

(158) Minemura, Y.; Ito, S.; Miyao, T.; Naito, S.; Tomishige, K.; Kunimori, K. *Chem. Commun.* **2005**, 1429−1431.

(159) Minemura, Y.; Kuriyama, M.; Ito, S.-I.; Tomishige, K.; Kunimori, K. *Catal. Commun.* **2006**, *7*, 623−626.

(160) Pedrero, C.; Waku, T.; Iglesia, E. *J. Catal.* **2005**, *233*, 242−255.

(161) Kuriyama, M.; Tanaka, H.; Ito, S.-I.; Kubota, T.; Miyao, T.; Naito, S.; Tomishige, K.; Kunimori, K. *J. Catal.* **2007**, *252*, 39−48.

(162) Tanaka, H.; Kuriyama, M.; Ishida, Y.; Ito, S.-I.; Tomishige, K.; Kunimori, K. *Appl. Catal., A* **2008**, *343*, 117−124.

(163) Tanaka, H.; Kuriyama, M.; Ishida, Y.; Ito, S.-I.; Kubota, T.; Miyao, T.; Naito, S.; Tomishige, K.; Kunimori, K. *Appl. Catal., A* **2008**, *343*, 125−133.

(164) Han, Y.-F.; Kahlich, M. J.; Kinne, M.; Behm, R. J. *Phys. Chem. Chem. Phys.* **2002**, *4*, 389−397.

(165) Kahlich, M. J.; Gasteiger, H. A.; Behm, R. J. *J. Catal.* **1997**, *171*, 93−105.

(166) Sirijaruphan, A.; Goodwin, J. G., Jr.; Rice, R. W. *J. Catal.* **2004**, *227*, 547−551.

(167) Xu, J.; Xu, X.-C.; Ouyang, L.; Yang, X.-J.; Mao, W.; Su, J. J.; Han, Y.-F. *J. Catal.* **2012**, *287*, 114−123.

(168) Atalik, B.; Uner, D. *J. Catal.* **2006**, *241*, 268−275.

(169) Joo, S. H.; Park, J. Y.; Renzas, J. R.; Butcher, D. R.; Huang, W. Y.; Somorjai, G. A. *Nano Lett.* **2010**, *10*, 2709−2913.

(170) van Santen, R. A. *Acc. Chem. Res.* **2009**, *42*, 57−66.

(171) Gracia, F. J.; Bollmann, L.; Wolf, E. E.; Miller, J. T.; Kropf, A. J. *J. Catal.* **2003**, *220*, 382−391.

(172) Guerrero, S.; Wolf, E. E. *Chem. Eng. Sci.* **2011**, *66*, 4477−4487.

(173) Li, L.; Wang, X.; Shen, J.; Zhou, L.; Zhang, T. *J. Therm. Anal. Calorim.* **2005**, *82*, 103−107.

(174) Mhadeshwar, A. B.; Vlachos, D. G. *J. Catal.* **2005**, *234*, 48−63.

(175) Liu, X. S.; Korotkikh, O.; Farrauto, R. *Appl. Catal., A* **2002**, *226*, 293−303.

(176) Widmann, D.; Liu., Y.; Schüth, F.; Behm, R. J. *J. Catal.* **2010**, *276*, 292−305.

(177) Widmann, D.; Behm, R. J. *Angew. Chem., Int. Ed.* **2011**, *50*, 10241−10245.

(178) Li, M. J.; Wu, Z. L.; Overbury, S. H. *J. Catal.* **2011**, *278*, 133−142.

(179) Siani, A.; Alexeev, O. S.; Lafaye, G.; Amiridis, M. D. *J. Catal.* **2009**, *266*, 26−38.

(180) Tanaka, K. I.; Shou, M.; He, H.; Shi, X. Y. *Catal. Lett.* **2006**, *110*, 185−190.

(181) Margitfalvi, J. L.; Borbáth, I.; Lázár, K.; Tfirst, E.; Szegedi, A.; Hegedűs, M.; Gőbölös, S. *J. Catal.* **2001**, *203*, 94−103.

(182) Sirijaruphan, A.; Goodwin, J. G., Jr.; Rice, R. W. *J. Catal.* **2004**, *224*, 304−313.

(183) Schubert, M. M.; Gasteiger, H. A.; Behm, R. J. *J. Catal.* **1997**, *172*, 256−258.

(184) Tanaka, K.; Moro-oka, Y.; Ishigure, K.; Yajima, T.; Okabe, Y.; Kato, Y.; Hamano, H.; Sekiya, S.; Tanaka, H.; Matsumoto, Y.; Koinuma, H.; He, H.; Zhang, C. B.; Feng, Q. C. *Catal. Lett.* **2004**, *92*, 115−121.

(185) Shou, M.; Tanaka, K.-I. *Catal. Lett.* **2006**, *111*, 115−118.

(186) Tanaka, K.; Shou, M.; He, H.; Shi, X. Y.; Zhang, X. L. *J. Phys. Chem. C* **2009**, *113*, 12427−12433.

(187) Tanaka, K.-I.; He, H.; Shou, M.; Shi, X. Y. *Catal. Today* **2011**, *175*, 467−470.

(188) Salomons, S.; Hayes, R. E.; Votsmeier, M. *Appl. Catal., A* **2009**, *352*, 27−34.

(189) Mhadeshwar, A. B.; Vlachos, D. G. *J. Phys. Chem. B* **2004**, *108*, 15246−15258.

(190) Grabow, L. C.; Gokhale, A. A.; Evans, S. T.; Dumesic, J. A.; Mavrikakis, M. *J. Phys. Chem. C* **2008**, *112*, 4608−4617.

(191) Zhai, Y. P.; Pierre, D.; Si, R.; Deng, W. L.; Ferrin, P.; Nilekar, A. U.; Peng, G. W.; Herron, J. A.; Bell, D. C.; Saltsburg, H.; Mavrikakis, M.; Flytzani-Stephanopoulos, M. *Science* **2010**, *329*, 1633−1636.

(192) Fukuoka, A.; Kimura, J.; Oshio, T.; Sakamoto, Y.; Ichikawa, M. *J. Am. Chem. Soc.* **2007**, *129*, 10120−10125.

(193) Huang, S. J.; Hara, K.; Okubo, Y.; Yanagi, M.; Nambu, H.; Fukuoka, A. *Appl. Catal., A* **2009**, *365*, 268−273.

(194) Herzing, A. A.; Kiely, C. J.; Carley, A. F.; Landon, P.; Hutchings, G. J. *Science* **2008**, *321*, 1331−1335.